Nanoscale

Accepted Manuscript

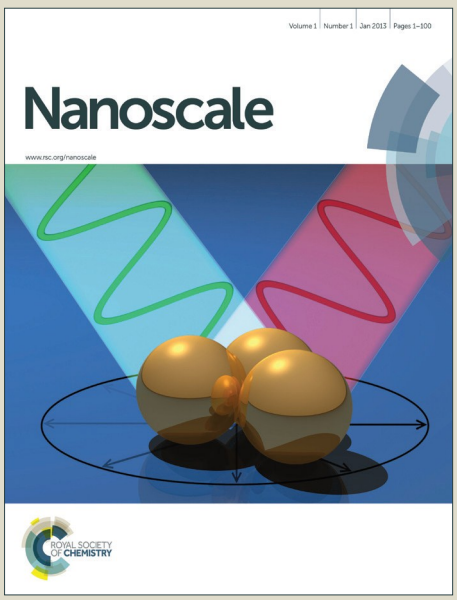

ROYAL SOCIETY OF CHEMISTRY

www.rsc.org/nanoscale

Cite this: DOI: 10.1039/c0xx00000x

www.rsc.org/xxxxxx

REVIEW

Polymeric AIE-based Nanoprobes for Biomedical Applications: Recent Advances and Perspectives

Xiaoyong Zhang[a,b,*], Ke Wang[b], Meiying Liu[a], Xiqi Zhang[b], Lei Tao[b], Yiwang Chen[a] and Yen Wei[b,*]

Received (in XXX, XXX) Xth XXXXXXXXX 20XX, Accepted Xth XXXXXXXXX 20XX

DOI: 10.1039/b000000x

The development of polymeric luminescent nanomaterials for biomedical applications has recently attracted great attention due to their remarkable advantages as compared with the small organic dyes and fluorescent inorganic nanomaterials. Among these polymeric luminescent nanomaterials, the polymeric luminescent nanomaterials based on dyes with aggregation induced emission (AIE) properties should be of great research interest for their unique AIE properties, designability of polymers and multifunctional potential. In this review, the recent advances in design and biomedical applications of polymeric luminescent nanomaterials based on AIE dyes is summarized. Various design strategies for incorporation of these AIE dyes into polymeric systems were included in this review article. Potential biomedical applictions such as biological imaging, biological sensor and theranostic systems of these polymeric AIE-based nanomaterials have also been highlighted. We trust this review will attracted great interest of scientists from different research fields in chemistry, materials, biology and interdiscipline.

1. Introduction

Nanomedicine is an emerging and fast growing field which mainly involves chemsitry, materials, biology and medicine.[1] The development of novel fluorescent nanomaterials for biomedical applications has become one of the most important aspects of nanomedicine and attracted increasing research interest.[2-5] Since the first report of semiconductor quantum dots for biological applications,[6] a vast of luminescent nanomaterials based on inorganic, organic and hybrid components have been developed due to their obvious advantages over small organic dyes. As compared with small organic dyes, fluorescent nanomaterials showed superior photostability, size tunable emission, multifunctional potential and desirable pharmacokinetic behavior. Thus, various fluorescent inorganic nanoparticles (FINs) such as semiconductor quantum dots, fluorescent carbon dots, Ln ions doped nanomaterials, photoluminescent silicon nanoparticles, metallic nanoclusters and polymeric luminescent nanoparticles have been developed and extensively investigated for diverse biomedical applications.[7-42] Previous studies have been mainly focused on the FINs and great progress has been made over the past few decades. However, the major issues for the practical biomedical applications of FINs, especially for *in vivo* applications, are still a forbidden challenge for their accumulation in reticuloendothelial system, difficult to be biodegradable and notorious toxicity to the living organisms.[43, 44] Therefore, a type of alternative luminescent nanomaterials, fluorescent organic nanoparticles (FONs) have recently emerged.

To date, a variety of FONs based on conventional organic dyes, conjugated polymers, boron-dipyrromethene based polymers, metal coordination luminescent polymers, fluorescent proteins and polydopamine *et al* have been developed.[16, 30, 45-90] As compared with FINs, the FONs have some distinct advantages for biomedical applications. 1) the organic dyes with different optical properties and functional groups can be arbitrarily designed according to the requirements. 2) these fluorescent dyes can be incorporated with a number of other functional components through different fabrication strategies. 3) FONs are composited with organic components, which are biocompatible and biodegradable potential. Because of these remarkable features, FONs have been used for different application fields ranged from biological sensor, drug delivery and diagnostic *et al*.[91-101] Despite great advance has been made, it is still a great challenge to fabricate FONs with strong fluorescent intensity. It is well known that most of dyes are hydrophobic nature, which is not suitable for biomedical applications. Therefore, these hydrophobic luminescent dyes should be first integrated with hydrophilic components to compatible with the biological system. During this procedure, the hydrophobic dyes were encapsulated in the core of FONs, and their fluorescence will be partial or almost completely decreased due to the notorious aggregation caused quenching (ACQ) effect. Therefore, searching for novel dyes that could overcome the ACQ effect is of utmost important for fabrication of ultrabright FONs.

Aggregation induced emission (AIE) or aggregation enhanced emission is distinctive fluorescence phenomenon, which suggested that some dyes can emit much stronger fluorescence in their aggregate or solid state than in dispersion solution. Different mechanism including J-aggregate formation, conformational planarization and twisted intramolecular charge transfer for the AIE phenomenon has been previously proposed by Tang et al. However, none of them could be fully supported by the experimental data.[102, 103] The unique AIE properties of these dyes made them very

promising for fabrication of ultrabright luminescent polymeric nanoparticles.[58, 78, 104-131] In recent years, increasing attention has been devoted toward the fabrication and biomedical applictions of these AIE dye based FONs.[132] In this review, recent advances in fabrication and biomedical applications of polymeric AIE dye based materials were summarized and discussed. Especially, the recent development of AIE dye based materials for theranostic applications will be highlighted.

2. Design strategies for polymeric AIE dye based nanoprobes

AIE dyes are a novel type of organic dyes which exhibited enhanced fluorescence in their aggregate state. Because of their unique AIE properties, fluorescent nanoparticles based on AIE dyes have recently attracted great research interest for fabrication of ultrabright nanoprobes. Over the past few years, different strategies for fabrication of AIE-based fluorescent nanoprobes have been developed. In this part, a number of design strategies for fabrication of polymeric AIE dye based nanoprobes were first introduced.

2.1 Self assembly of AIE dyes and amphiphilic polymers

Polymeric micelles usually constituted with hydrophobic inner core and hydrophilic outer shell. These polymeric micelles were formed through self-assembly of amphiphilic block copolymers in aqueous solution.[133-141] In 2010, *Jen* et al reported a non-covalent method for coencapsulation of two AIE dyes (1,1,2,3,4,5-hexaphenylsilole (HPS) and/or bis(4-(N-(1-naphthyl) phenylamino)-phenyl)fumaronitrile (NPAFN)) into three amphiphilic block compolymers (**Fig. 1**).[142] Among these micelles, the fluorescence resonance energy transfer from the green-mitting donor (HPS) to the red-emitting acceptor (NPAFN) was explored. The cell imaging application and biocompatibility of these AIE dye based micelles have also been investigated. They demonstrated that high fluorescence quantum yield and prolonged fluorescence lifetime of HPS could be achieved by encapsulating HPS in the micelles. The improved fluorescence properties of HPS can be ascribed to the restricted intramolecular rotation of the dyes in hydrophobic core environment of micelles. More importantly, the micelles could also prevent the aggregation of AIE dyes in aqueous media, which made them useful for biomedical applications.

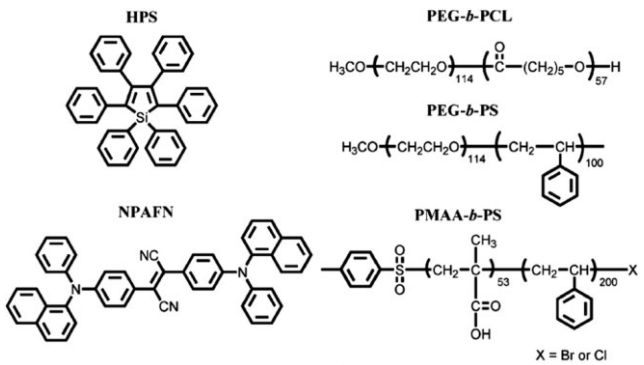

Fig. 1 Preparation of AIE dye based nanoprobes via non-covalent self assembly between AIE dyes and amphiphilic copolymers. Chemical structures of AIE dyes (named as HPS and NPAFN) and amphiphilic block copolymers. (Reprinted with permission from Ref. [142])

Pluronic F127 is a commercial available non-ionic surfactant, that is composited with two hydrophilic segments and a hydrophobic segment. In recent years, we have developed a rather simple strategy for fabrication of AIE dye based bioprobes via self assembly of an AIE dye An18 (derivatized from 9,10-distyrylanthracene with two alkoxyl end groups) and F127. The An18 contained FONs can be facilely obtained via mixing of An18 and F127 in the mixture solvents of tetrahydrofuran (THF) and water. After removal of THF, An18 was encapsulated in FONs and showed high water dispersibility and excellent biocompatibility, making them highly potential for bioimaging applications (**Fig. 2**).[143] Apart from F127, other commercialized biocompatible surfactants such as lecithin could also be combined with the AIE dyes, which provided a facile and effective strategy to fabricate water-soluble polymeric AIE dye based nanoprobes for biological applications.[144, 145]

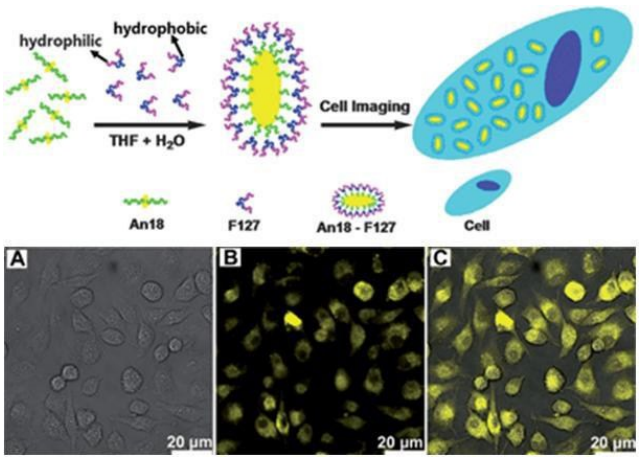

Fig. 2 Fabrication and biological imaging applications of An18-F127 via self assembly of An18 and commercial available surfactant (F127). Schematic showing transformation of An18 from hydrophobic to hydrophilic fluorescent nanoparticles with Pluronic F127 and their use as cell imaging probes. And cell imaging of An18-127 nanoparticles using CSLM (A) bright field, (B) 405 nm excitations, (C) overlay of image A and B. (Reprinted with permission from Ref. [143])

As compared with commercial available amphiphilic polymers, synthetic polymers could be finely tuned their properties via choosing different monomers and adjusting the ratio of hydrophobic and hydrophilic segments. In a recent report, we found that PEGylated AIE dye based FONs could be obtained through mixing AIE active materials (An18) and synthetic polymers poly((stearyl methacrylate) SMA-*co*-poly(ethylene glycol) methacrylate (PEGMA)), which were synthesized from reversible addition fragmentation chain transfer (RAFT) polymerization using SMA and PEGMA as monomers.[146] The particle size of these PEGylated FONs is less than 100 nm, which is much smaller than that of F127 encapsulated AIE dye based FONs. More importantly, many functional groups could also be facilely integrated into these AIE dye based FONs via using different monomers. Thus fabrication of AIE dye based polymeric nanoparobes through self assembly of synthetic polymers and AIE dyes should be

of great research interest owing to the designability of the synthetic polymers. Furthermore, other functional components could also be introduced into AIE dye based polymeric systems via self assembled AIE dyes with two different amphiphilic polymers with functional groups, which could be futher linked with targeting agents for specific bioimaging applications. For example, Liu *et al* have reported that folate acid functionalized AIE dye based FONs could be obtained via self assembly of AIE dyes (TPE-TPA-DCM) with a mixture of lipid derivatives, DSPE-PEG2000 and DSPE-PEG5000-folate simultaneously.[147] The targeting capability of the obtained FONs toward the folate receptor positive cancer cells and tumors was investigated. They demonstrated that these folate acid functionalized AIE dye based nanoprobes can be mainly internalized by MCF-7 cancer cells through caveolae-mediated endocytosis. More importantly, these AIE dye based FONs can be effectively accumulated in tumor. These results suggested that targeting agents functionalized AIE dye based nanoprobes are promising for biological imaging applications.

2.2 Covalent linkage of AIE dyes with polymers

Covalent linkage of AIE dyes with hydrophilic segments is another important strategy for fabrication of AIE dye based nanoprobes.[148] In 2013, we have developed a novel covalent strategy for fabrication of AIE dye based polymeric nanoprobes via Schiff base condensation between the AIE dye (named as P5) with aldehyde group and natural polysaccharide chitosan with a number of amino groups **(Fig. 3**).[149, 150] It is well known that the aldehyde and amino groups can form Schiff base under alkaline environment. In this work, we just need mixing the aldehyde-contained AIE dye and chitosan in one-pot and then condensation reduction of the Schiff base to afford stable linkage of AIE dye and chitosan using $NaBH_4$. Because a large number of carboxyl and hydroxyl groups were existed on chitosan, the P5-chitosan FONs showed amphiphilic properties. After removal of the organic solvent (THF), these amphiphilic compounds could self assemble into AIE nanoprobes. Because of the strong fluroescence of the P5-chitosan FONs, a very low concentration of these nanoprobes can light up the cells very well. On the other hand, the free carboxyl groups could also be used for further conjugation of other components to P5-chitosan FONs. Thus multifunctional AIE dye based nanotherapeutic system may also be fabricated.

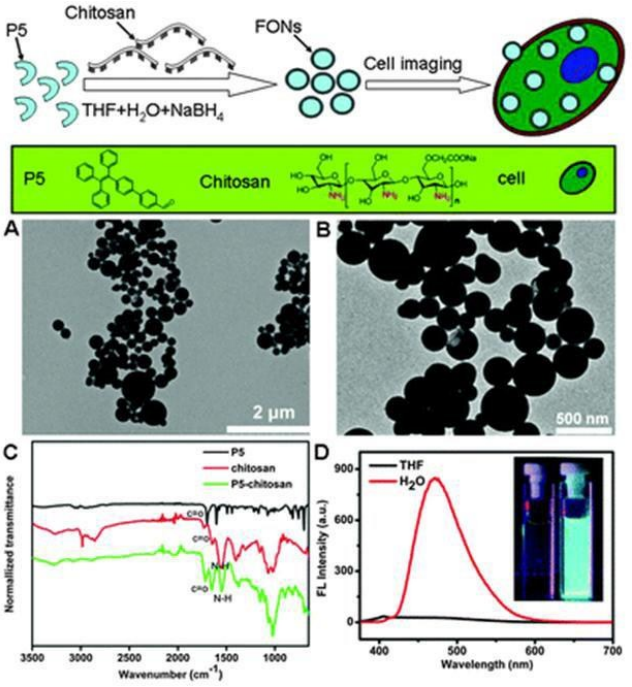

Fig. 3 Schematic showing the preparation of P5–chitosan FONs based on Schiff-based condensation, and their cell imaging applications. Characterization of P5, chitosan and the P5–chitosan FONs. (A and B) TEM images of the P5–chitosan FONs; the images show that the diameters of the P5–chitosan FONs range from 200–400 nm. (C) Normalized IR spectra of P5, chitosan and the P5–chitosan FONs. Strong C=O stretching vibration bands located at 1730 cm^{-1} and C–O stretching vibration bands located at 1100 cm^{-1} are observed for the P5–chitosan FONs, suggesting P5–chitosan FONs are formed. (D) PL spectra of P5 (THF) and the P5–chitosan FONs (H_2O), with an excitation wavelength of 365 nm. The insets are fluorescent images of dispersed P5 (THF, left cuvette) and P5–chitosan FONs (H_2O, right cuvette) under a UV lamp (λ = 365 nm). (Reprinted with permission from Ref. [149])

2.3 Emulsion polymerization

Polymerization is a typical strategy for fabrication of nanomaterials for biomedical applications. A number of polymerization methods, which include atom transfer radical polymerization (ATRP), Ring-opening polymerization (ROP), RAFT polymerization, nitroxide mediated radical polymerization (NMP), single electron transfer living radical polymerization (SET-LRP), emulsion polymerizaiton, ring-opening metathesis polymerization (ROMP) and free radical polymerization have been developed over the past few decades.[42, 72, 103, 151-192] In the past few years, many of these polymerization methods were utilized for preparation of AIE dye based polymeric nanoprobes. For example, we have recently developed a rather facile and effective method for preparation of AIE dye based nanoprobes via emulsion polymerization (**Fig. 4**).[193] In this procedure, a polymerizable AIE dye (named as PhE) was copolymerized with styrene and acrylic acid in the present of surfactant (sodium dodecyl sulfate). And the polymerization was initiated by ammonium persulfate in aqueous solution. After successful polymerization, the obtained polymers contained PhE, styrene and acrylic acid showed amphiphilic properties, that will be self assembled into AIE dye based nanoprobes in aqueous

solution. These polymeric AIE nanoprobes exihibited small size, uniform morphology, high water dispersibility and excellent biocompatibility. More importantly, a large number of hydrophilic carboxyl groups were introduced on the surface of these polymeric AIE nanoprobes. The introduction of carboxyl groups provide the potential for further surface modification of these polymeric AIE nanoprobes with other functional components, which will be very important for the biomedical applications.

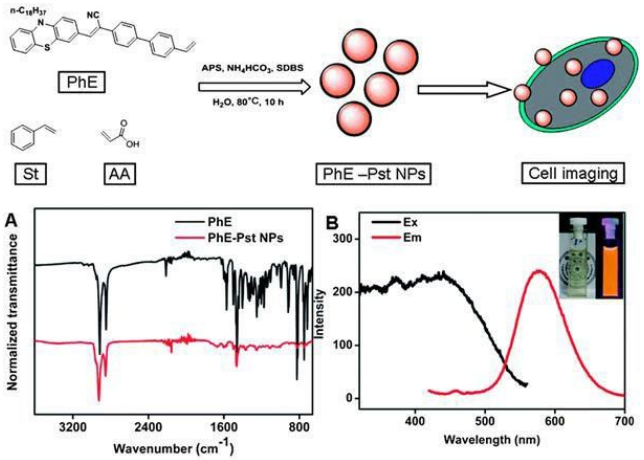

Fig. 4 Preparation of PhE-Pst NPs through emulsion polymerization. Schematic showing the preparation of PhE–Pst NPs and their cell imaging applications. (A) FT-IR spectra and (B) PL spectra of PhE, PhE–Pst NPs. The inset of (B) shows the aqueous solution of PhE–Pst NPs in daylight (left cuvette) and when irradiated by a UV lamp at 365 nm (right cuvette). (Reprinted with permission from Ref. [193])

2.4 RAFT polymerization

RAFT polymerization is one kind of reversible deactivation radical polymerizations, which was first discovered at the commonwealth scientific and industrial research organisation in 1998. In general, thiocarbonylthio compounds were used as chain transfer agents (CTA) to afford control over the generated molecular weight and polydispersity during a free radical polymerization. In one of our recent reports, we demonstrated that a polymerizable AIE dye (PhE) can be copolymerized with a biocompatible and hydrophilic monomer (PEGMMA) using a carboxyl group contained CTA. Results demonstrated that the macromolecular weight and polydispersity of the obtained polymers can be well controlled through RAFT polymerization (**Fig. 5**).[194] The molecular weights (Mn) of the copolymers were 17470 and 24436 Da, with narrow polydispersity indices of 1.16 and 1.12 for PhE–PEG-20 and PhE–PEG-40, respectively. These polymers can be self-assembled into spherical nanoparticles with size range from 100-200 nm. Due to their strong fluorescence, high water dispersiblity and excellent biocompatibility, these AIE nanoprobes exhibited good performance for cell imaging applications. The copolymerization of other AIE dyes with different monomers were also reported by many other groups. These results also suggested that well controlled AIE dye contained polymers could be prepared from RAFT polymerization, that are promising for bioimaging applications.[81, 195]

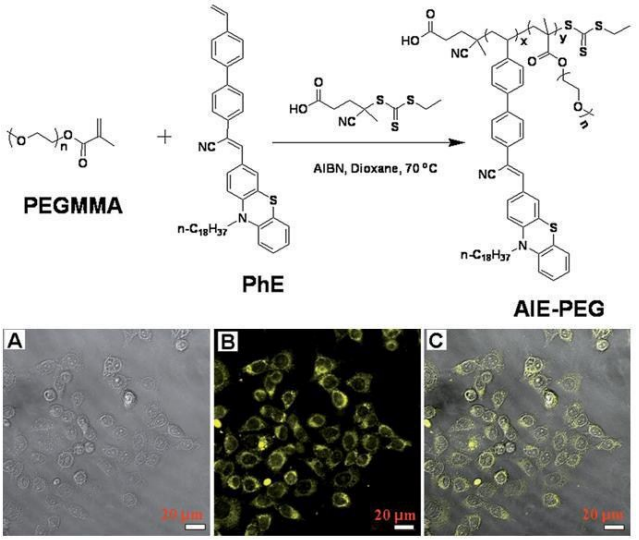

Fig. 5 Synthesis of PhE based FONs *via* RAFT polymerization, based on the designed DP; thus obtained FONs were named PhE–PEG-20 (DP = 20) and PhE–PEG-40 (DP = 40). CLSM images of A549 cells incubated with 40 μg mL^{-1} of PhE–PEG-20 for 3 h. (A) Bright field image, (B) excited with a 488 nm laser, and (C) merged image of A and B. Scale bar = 20 μm. (Reprinted with permission from Ref. [194])

The stability of amphiphilic copolymers in diluted aqueous solution is very important for their practical biomedical applications.[75, 132, 196-201] A general strategy to improve the stability of these amphiphilic copolymers is to incorporate a cross-linker in these copolymers. In our recent report, a novel cross-linked AIE dye contained copolymers were prepared via RAFT polymerization. In this work, the AIE dye bearing with hydroxyl group was first conjugated with carboxyl group of CTA to obtain the AIE dye contained CTA (P4-CTA). And then the monomers PEGMA and DEGDM were copolymerized through RAFT polymerization initiated from P4-CTA (**Fig. 6**).[196] The obtained cross-linked AIE dye based copolymers showed excellent water dispersibility, enhanced fluorescent intensity and low critical micelle concentrations (CMC). The CMC determined by the fluroescence intensity change of these AIE copolymers are 0.178 and 0.155 mg mL^{-1} for P4-PEG-1 and P4-PEG-2, respectively. However, we can still detect signals by dynamic laser scattering when the concentrations of P4-PEG were less than 0.1 μg mL^{-1}, implying the excellent stability of P4-PEG FONs in aqueous solution. Based on this concept, many other cross-linked polymeric AIE nanoprobes were also fabricated via similar strategy.[202] As compared with the noncross-linked polymeric nanoparticles, The cross-linked polymeric AIE dye based nanoprobes should be more suitable for practical biomedical applications because they could overcome the stability issue of noncross-linked micelles in diluted solution.

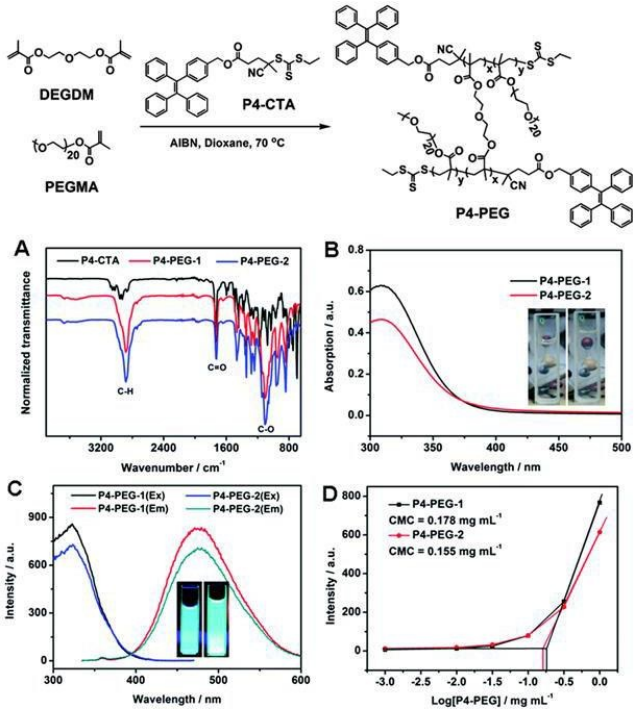

Fig. 6 Preparation of cross-linked P4-PEG FONs through RAFT polymerization. Synthetic routes of P4-PEG: RAFT polymerization of a hydrophilic monomer (PEGMA) and a cross-linker dimer (DEGDM) with a new AIE chain transfer agent (P4-CTA) to afford P4-PEG. (A) Normalized IR spectra of P4-CTA, P4-PEG-1 and P4-PEG-2. Strong alkyl C–H stretching vibration located at 1880 cm^{-1} and C–O stretching vibration bands, which are located at 1103 cm^{-1}, were observed in the sample of P4-PEG FPNs, suggesting their successful preparation. (B) UV absorption spectra of P4-PEG FPNs dispersed in water. Inset: visible images of P4-PEG-1 (left) and P4-PEG-2(right) FPNs in water. (C) Fluorescence excitation (Ex) and emission (Em) spectra of P4-PEG FPNs, inset are fluorescent images of P4-PEG-1 (left) and P4-PEG-2 (right) FPNs taken under 365 nm of UV light. (D) Intensity of the aggregate emission vs. the logarithm of the concentration of P4-PEG (λex = 405 nm, λem = 477 nm). (Reprinted with permission from Ref. [196])

2.5 Ring-opening metathesis polymerization

ROMP is a type of olefin metathesis chain-growth polymerization that used for prepration of industrially important products. The reaction uses strained cyclic olefins to obtain steroregular and monodisperse polymers and copolymers. The driving force for the ROMP is the relief of ring strain. As compared with standard polymerization methods, the obvious advantages of ROMP is the obtained polymers typically possess a very narrow range of molecular weights. Another important characteristic of ROMP systems is typically living polymerization catalysts. Therefore ROMP is a superior method for preparing diblock and triblock copolymers with define functional groups. Because of these features, Zhang *et al* have investigated the preparation of AIE dye based nanoprobes via ROMP. As shown in **Fig. 7**, amino functionalized AIE dye and PEG were first reacted with cis-5-norbornene-exo-2,3-dicarboxylic anhydride through the ring-opening reaction. And then these monomers named as M1 and M2 were sequentially polymerized using the third generation Grubbs' catalyst (G3) as initiator via ROMP. These obtained AIE contained copolymers can be self-assembled into nanoparticles with different morphology via adjusting the polymerization conditions. On the other hand, all the polymers showed very narrow molecular weights with PDI less than 1.1. More importantly, these well-defined polymers can be fastly produced at room temperature even opening in air. Despite these advantages, only one report has demonstrated the preparation of AIE dye based polymers through ROMP. We trust that the ROMP should be a very promising strategy for fabrication of well controlled polymeric AIE dye based nanoprobes as the following issues such as cost of Grubbs' catalyst and applicability of monomers were overcomed.

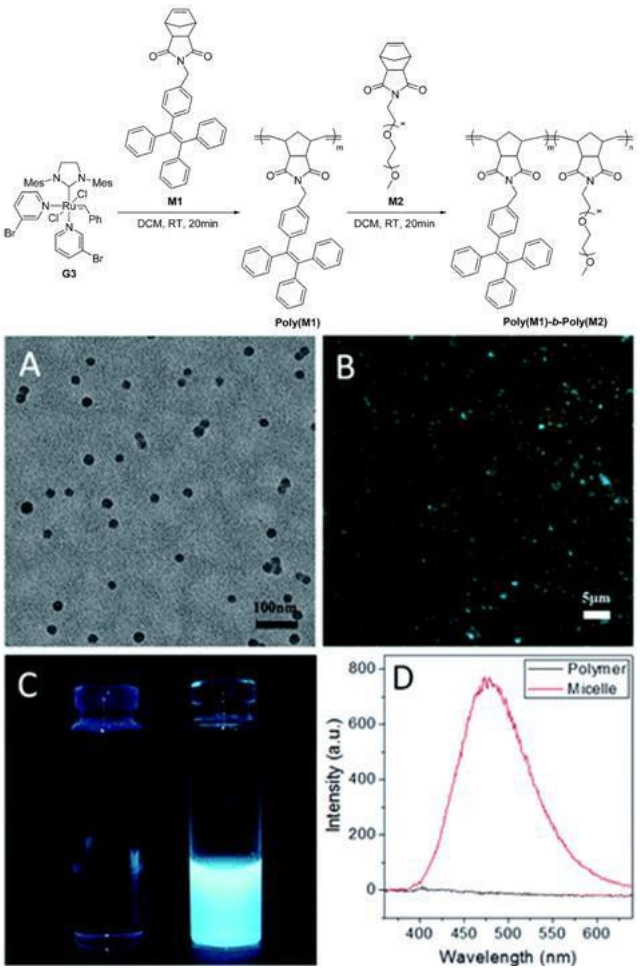

Fig. 7 Fabrication of AIE dye based copolymers via ROMP. The preparation of AIE amphiphilic diblock copolymer of poly(M1)-b-poly(M2). (A) TEM image and (B) fluorescence microscope image of the spherical micelles formed from poly$(M1)_{50}$-b-poly$(M2)_{10}$. (C) Pictures of the poly$(M1)_{50}$-b-poly$(M2)_{10}$ THF solution (left) and the resultant micelle dispersion in mixed THF and water (v/v = 1/4) (right). (D) Fluorescence spectra of the poly$(M1)_{50}$-b-poly$(M2)_{10}$ THF solution (black) and the resultant micelle dispersion in water (red). (Reprinted with permission from Ref. [203])

2.6 Polymerization through ring-opening reaction

Recently, a rather facile strategy for preparation of AIE dye based polymers has been developed by our group. The strategy is based on the ring-opening reaction between anhydride and amino compounds.[73] For example, we have recently demonstrated that glucose terminated amphiphilic copolymers can be prepared through ring-opening reaction

between the AIE dye with two amino groups and agents with two anhydride groups (**Fig. 8**).[189] The ring-opening reaction can be occurred under rather mild conditions such as room temperature, within a few minutes, without protection by inert gas and not requirement of catalysts. On the other hand, a large number of carboxyl groups were introduced in the copolymers during ring-opening reaction. These hydrophilic groups not only enhanced the water dispersibility of the obtained copolymers, but also provided active sites for further reaction and complexing with drugs. Many other components such as amino PEG and other compounds could also be introduced to the copolymers through ring-opening reaction.[132, 165, 204, 205] Finally, the ring-opening between anhydride and amino groups can also be extended for fabrication of more smart copolymers via combination of two or more fabrication strategies.

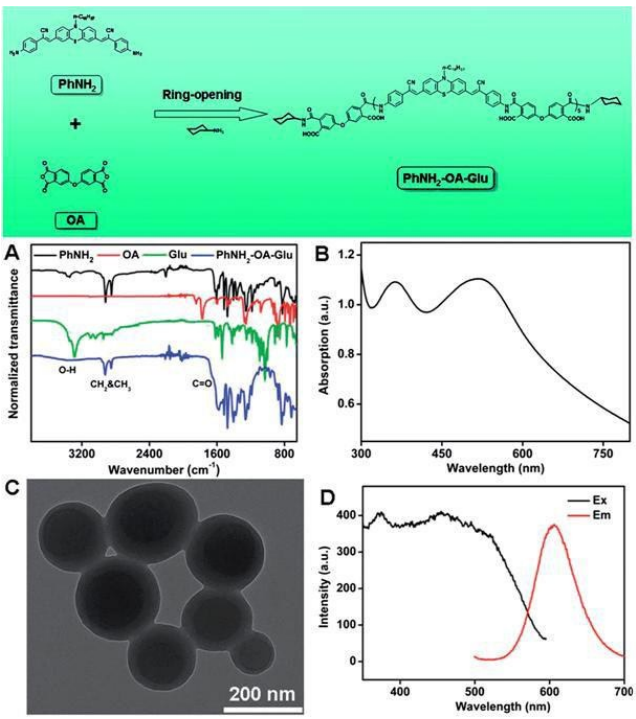

Fig. 8 Fabrication of AIE dyes-containing gluocopolymers via ring-opening reaction. Schematic showing the preparation of glycosylated $PhNH_2$–OA–Glu FONs through ring-opening polymerization (ROP) and cell imaging applications of $PhNH_2$–OA–Glu FONs. Characterization of $PhNH_2$ and $PhNH_2$–OA–Glu FONs, (A) normalized IR spectra of $PhNH_2$, OA, Glu and $PhNH_2$–OA–Glu FONs, strong stretching vibration bands of C=O which located at 1732 cm^{-1} and C–O stretching vibration bands which located at 1108 cm^{-1} were observed in the sample of $PhNH_2$–OA–Glu FONs, suggesting $PhNH_2$–OA–Glu FONs were successfully fabricated. (B) UV-Vis spectrum of $PhNH_2$–OA–Glu FONs. (C) TEM images of **$PhNH_2$–OA–Glu** FONs; images showed that the diameters of $PhNH_2$–OA–Glu FONs are about 100–200 nm. (D) PL spectra of $PhNH_2$–OA–Glu (in water), the emission wavelength of $PhNH_2$–OA–Glu FONs is 600 nm. The excitation spectra showed that the excitation wavelength is very broad. (Reprinted with permission from Ref. [189])

2.6 Sol-gel encapsulation

Silica nanoparticles are a type of inorganic polymeric nanomaterials, that can be prepared via hydrolysis of silica precursors under alkaline or acid solution. Because of controllable synthesis, easy surface modification and excellent physicochemical properties such as good hydrophiphilicity, optical transparence and biocompatibility, silica nanoparticles have been extensively explored for various biomedical applications.[206-212] Among them, the encapsulation of dyes into silica matrix to obtain luminescent silica nanoparticles has attracted great research attention.[213-219] As the dyes were encapsulated into the silica nanoparticles, the dyes were aggregated in the core, however their surface was covered by silica shell, which can serve as a protective shield for improving the fluorescent stability of these dyes. Although great achievement has been made in preparation and biomedical imaging applications of these luminescent silica nanoparticles, it is still difficult to prepare ultrabright silica nanoprobes because of the ACQ effect of conventional organic dyes. In a recent report, Tang et al have demonstrated that the AIE dyes (TPE and silole derivates) can be conjugated with silica precursors, which were hydrolysized with other silica precursors through stöber method for preparation of luminescent silica nanoparticles contained AIE dyes (**Fig. 9**).[220] Through adjusting the synthesis parameters, the size of these AIE dye based luminescent silica nanoparticles (FSNP-1 and FSNP-2) can be well controlled. Results showed that these luminescent silica nanoparticles showed well dispersibility, strong fluorescent intensity and excellent biocompatibility, that are very suitable for biological imaging applications. On the other hand, the encapsulation of AIE dyes in other inorganic nanoparticles, such as zirconium phosphate nanoplatelets and hydroxyapatite has also been demonstrated recently.[221-223]

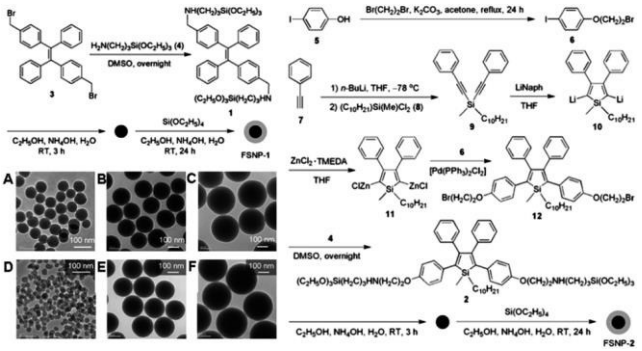

Fig. 9 Fabrication of TPE-containing fluorescent silica nanoparticle **FSNP-1** and silole-containing fluorescent silica nanoparticle **FSNP-2**. TEM images of monodispersed **FSNP-1** (A–C) and **FSNP-2** (D–F). Abbreviation: TPE = tetraphenylethene, DMSO = dimethyl sulfoxide, Naph = 1-naphthyl, THF = tetrahydrofuran, and TMEDA = *N*,*N*,*N*′,*N*′-tetramethylethylenediamine.(Reprinted with permission from Ref. [220])

The fabrication of AIE dye based luminescent silica nanoparticles via noncovalent encapsulation strategy has also been developed by our group. As shown in **Fig. 10**, the AIE dye (An18) was self-assembled with a silica percursor with alkyl chain (C18-Si) first in a mixture of THF and water. And then another silica precursor (TEOS) was added to cover on the AIE aggregates through stöber method.[224] After successful coating silica shell on the AIE aggregates, the luminescent silica nanoparticles were obtained. These luminescent silica nanoparticles exhibited uniform spherical morphology, strong

fluorescence, nontoxic and good performance for biological imaging applications. As compared with the covalent strategy, the noncovalent strategy need not specific functional groups and complex conjugation reaction to synthesize AIE dye containing silica precursors. Therefore it should be a rather facile and general strategy for fabrication of AIE dye based luminescent silica nanoparticles.

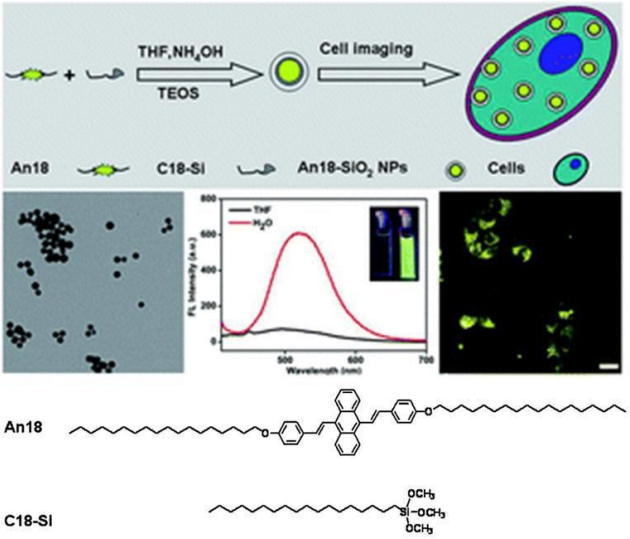

Fig. 10 Preparation and bioimaging applications of An18- silica nanoparticles through noncovalent strategy. Schematic showing the preparation of luminescent silica nanoparticles **(**An18-SiO_2 NPs**)** and their utilization for cell imaging applications. TEM images of the An18-SiO_2 NPs at different magnifications (left image). FL spectra of An18 in THF (black line) and An18-SiO_2 NPs in H_2O (red line). The inset shows a photograph of the An18 in THF (left cuvette) and An18-SiO_2 NPs in H_2O (right cuvette). The concentrations of An18 and the An18-SiO_2 NPs are 10 and 50 μg mL^{-1}, respectively (middle image). Confocal imaging of A549 cells. Cells were incubated with 10 μg mL^{-1} of An18-SiO_2 NPs for 3 h. The laser excitation wavelength was 488 nm (right image). (Reprinted with permission from Ref. [224])

3. Biomedical applications

The biomedical applications of AIE dye based nanoprobes have raised increasing attention in recent years. As compared with conventional fluorescent nanoprobes, the AIE dye based nanoprobes are of some obvious advantages such as strong fluorescent intensity, designability of AIE dyes, abundant fabrication methods and multifunctional potential. In the following section, the biomedical applications of AIE dye based nanoprobes for biological imaging, biological sensor and theranostics are summarized.

3.1 Biological imaging

Biological imaging is an important tool that could provide critical information for understanding various physiological and pathological processes, which are very useful for a number of biological applications such as cancer detection and treatment, stem cell transplantation，immunogenicity and tissue engineering. Over the past few decades, different biological imaging modalities, such as single photon emission computing tomography, magnetic resonances imaging, and positron emission tomography and fluorescence imaging have been developed.[62, 106, 192, 195, 225-247] Among them, biological imaging using fluorescence as signal output has attracted great research interest due to its advantages, including high resolution at subcellular levels, strong signal intensity, uncomplicated apparatus, biocompatibility and desinability of the fluroescent nanoprobes. The AIE dyes have recently been extensively explored for fabrication of ultrabright fluorescence nanoprobes for biological imaging. As an emerged type of fluorescent nanoprobes, many research attention has been made in the fabrication of AIE dye based nanoprobes for non-targeted biological applications.[248, 249] For example, Tang et al have recently demonstrated that water soluble and biocompatible AIE dye based nanoprobes can be fabricated via encapsulation a red emssion AIE dye (TPE-TPA-DCM) into bovine serum albumin (BSA) and then cross-linked by glutaraldehyde (**Fig. 11**).[250] These AIE dye based nanoprobes showed spherical morphology with diameter less than 100 nm. Due to their AIE properties, these fluorogen-loaded BSA NPs showed strong fluorescence and can be utilized for non-targeting biological imaging *in vitro* and *in vivo*. Futhermore, many other AIE dye based nanoprobes have also been fabricated via encapsulated AIE dyes into natural and synthetic polymers for non-targeting imaging applications.

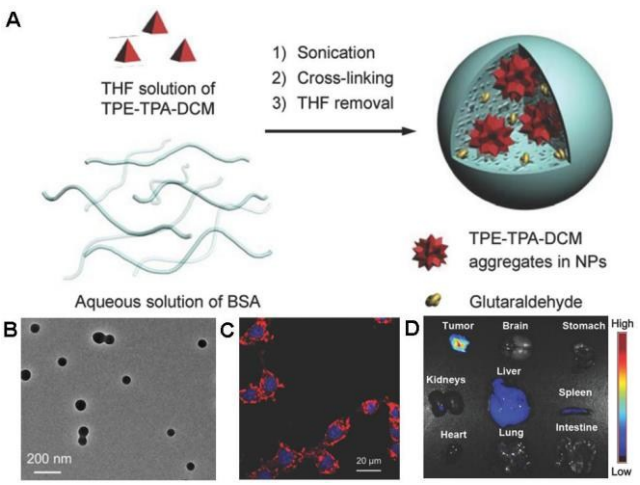

Fig. 11 (A) Schematic illustration of the fabrication of BSA NPs loaded with TPE-TPA-DCM. (B) TEM images of the AIE-active fluorogen-loaded BSA NPs. (C) CLSM images of MCF-7 breast cancer cells after incubation with fluorogen-loaded BSA NPs (with a fluorogen loading of 0.86%) for 2 h at 37 °C. [TPE-TPA-DCM] = 0.4 × 10^{-6} M. (D) Ex vivo fluorescence imaging on tumor tissue and major organs of mice treated with AIE-fluorogen-loaded BSA NPs, which were sacrificed at 24 h post-injection. The tissue autofluorescence was removed by spectral unmixing software. (Reprinted with permission from Ref. [250])

Apart from the non-targeting biological imaging, the targeting imaging using AIE dye based nanoprobes can be achieved via surface conjugation targeting agents such as folic acid, antibodies and peptides et al with AIE dye based nanoprobes, which showed targeting capability both *in vitro* and *in vivo*. For example, Huang et al have demonstrated that a series of metal complexes with different N^O ligands can be utilized for fabrication of luminescent nanoprobes via emulsion polymerization.[251] And then these AIE dye based nanoprobes were used for targeting biological imaging applications. As shown in **Fig. 12**, a series of Pt complexes with AIE properties can be incorporated into an amphiphilic polymers via free radical polymerization. And then their surface was conjugated with folic acid. The

targeting capability of these Pt complexes nanoprobes was indentified by comparsion of their cell uptake capability in the present and absent of folic acid. Results demonstrated that cell uptake of these Pt containing nanoprobes in the present of free folic acid is significant less than that of absent of folic acid (**Fig. 12b** and **Fig. 12c**). Except from folic acid, many other targeting agents have also been used for fabrication of AIE dye based nanoprobes with targeting capability.

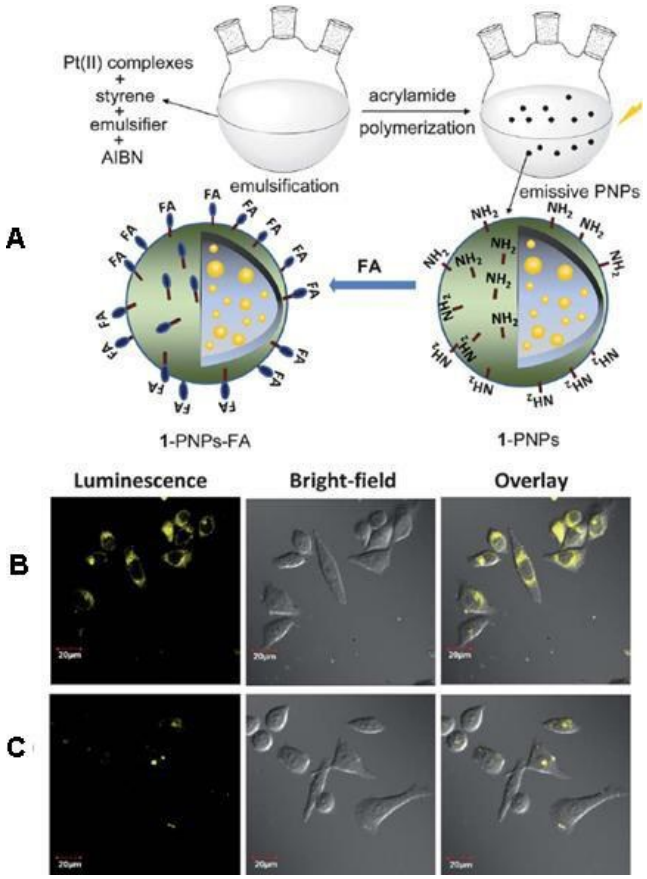

Fig. 12 (A) Synthesis of 1-PNPs-FA. (B) Luminescence images of HeLa cells incubated with 0.2 mg mL^{-1} 1-PNPs-FA for 30 min. (C) Luminescence images of HeLa cells incubated with 3 mM free folic acid for 2 h and then further incubated with 0.2 mg mL^{-1} 1-PNPs-FA for 30 min. (Reprinted with permission from Ref. [251])

Long term cell tracking is a very important method for understanding many biological behaviors such as cell migration, proliferation and differentiation, chemotaxis, and many other fundamental biological processes.[148, 252-256] In a recent report by Liu et al, alternative cell tracking nanoprobes based on AIE dyes have been fabricated via self assembly of BTPEBT and DSPE-PEG2000/DSPE-PEG2000-Mal. The obtained AIE dots were further conjugated with a targeting peptide (Tat) (**Fig. 13**).[257] Through the simple self-assembly of hydrophobic AIE dye (BTPEBT) and amphiphilic copolymers (DSPE-PEG2000/DSPE-PEG2000-Mal), water stable and biocompatible AIE dots can be obtained.

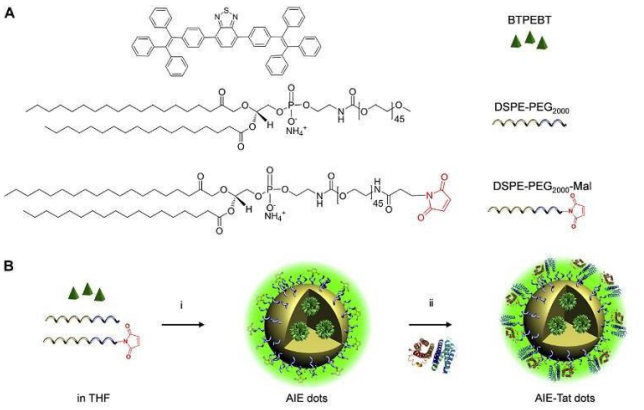

Fig. 13 (A) Chemical structures of BTPEBT, DSPE-PEG2000 and DSPE-PEG2000-Mal. (B) Schematic illustration of AIE-Tat dots formation. (Reprinted with permission from Ref. [257])

The continuous cell labeling by GFP and AIE-Tat dots were monitored by flow cytometry histograms and CLSM using HEK 293T cells. Results showed that the labeling efficiency of AIE-dots is as high as 99.98% at 1st day. The labeling efficiency still remains greater than 90% on the 5th day of post-incubation with AIE-dots. The clearly distinguishable fluorescent profile can still be observed after 10 days continuous cell culture as compared with the untreated cells (**Fig. 14A**). However, the highest GFP labeling rate is about 68% on the 1st day. No obvious difference was found on the 5th day as compared with blank cells. On the other hand, it can be seen that more than 50% cells show bright GFP fluorescence on the first two days, but only a few cells show GFP fluorescence on the 3rd and 5th day (**Fig. 14E**). These results suggested that the cell tracking performance of AIE-Tat dots is better than that of GFP plasmid transfection method. More importantly, multifunctional nanotheranostic systems can also be fabricated after the AIE-dots were conjugated with other funcitonal components such other targeting moieties and other imaging modilities.

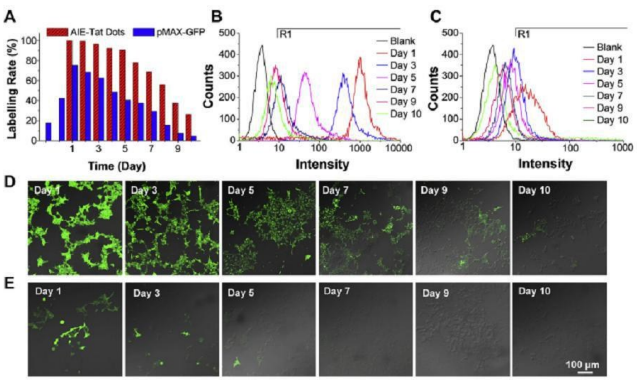

Fig. 14 (A) Continuous monitoring of cell labeling rates by GFP or AIE-Tat dots for 10 days. (B) and (C) Flow cytometry histograms of HEK 293T cells after incubation with 2 nM AIE-Tat dots (B) or 5 mg/well p-MAX-GFP plasmid (C) overnight and then sub-cultured for designated times. (D) and (E) CLSM images of HEK 293T cells labeled by AIE-Tat dots (D) or pMAX-GFP (E) at different days post-incubation. All the images share the same scale bar. (Reprinted with permission from Ref. [257])

Simultaneous detection of multibiotargets using different fluorescent nanoprobes upon a single laser excitation process great merits such as reduction of test time, instrument

complexity and cost as compared with the multiple laser setup. The desirable fluorescent nanoprobes for dual or multi-color imaging should be of good biocompatibility, high photostability, strong fluorescent intensity, large strokes shift, and more importantly, can be effectively excited using single laser.[258] In a recent reported by Liu et al, dual color biological imaging was achieved by using two AIE dye based nanoprobes with different fluorescent emission (**Fig. 15**).[258] These AIE dye based nanoprobes were prepared via nanoprecipitation method using AIE fluorogens as the fluorescent domain and biocompatible distearoyl-sn-glycero-3-phosphoethanolamine-poly(ethylene glycol) (DSPE-PEG) derivatives as the encapsulation matrix. And then the targeting agent (Tat peptide) was conjugated on the surface of AIE dye based nanoprobes to endow them targeting properties. These AIE dye based nanoprobes showed spherical morphology with average size about 30 nm based on TEM images (**Fig. 15a and b**). The two AIE dye based nanoprobes (GT-AIE and RT-AIE) showed intense absorption at the 455 nm and different emission peaks at 539 and 670 nm with minimized fluorescence spectral overlap (**Fig. 15c**). More importantly, the quantum yields of GT-AIE and RT-AIE dots in water were measured to be 58 and 25% using rhodamine 6G in ethanol (95%) and 4-(dicyanomethylene)-2-methyl-6-(p-dimethylaminostyryl)-4H-pyran in methanol (43%) as the references, respectively. These luminescent properties of the two AIE dye based nanoprobes made them desirable candidates for dual color biological imaging applications. *In vitro* andd *in vivo* biological imaging studies using the two AIE dye based nanoprobes were further evaluated. *In vitro* imaging results suggested that these Tat-funcitonalized AIE dots are able to label and simultaneously track the migration and interaction of two populations of cancer cells. *In vivo* imaging results demonstrated that different cell populations can be effectively descriminated when the cell mixture labeled with two AIE dots were intravenously injected into mice. The dual color biological imaging maybe important for various physiological and pathological procedures.

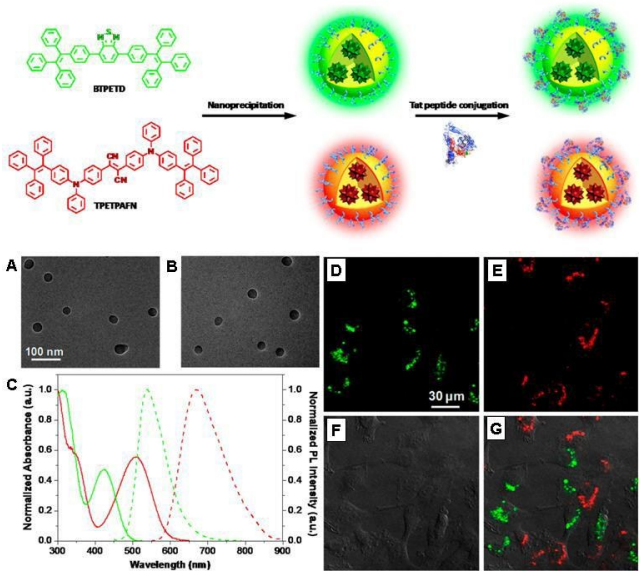

Fig. 15 Schematic illustration of synthesis of Tat-Functionalized AIE Dots. HR-TEM images of (A) GT-AIE and (B) RT-AIE dots. (C) UV–vis absorption (solid) and PL (dashed) spectra of GT-AIE (green) and RT-AIE (red) dots in water. Simultaneous monitoring of HT1080 fibrosarcoma cells labeled with 2 nM of either GT-AIE or RT-AIE dots after coculture for 12 h. Images are recorded under excitation at 458 nm with (D) 480–560 and (E) 670–800 nm bandpass filters. (F) Transmission image. (G) Fluorescence/transmission overlay image. (Reprinted with permission from Ref. [258])

Although fluorescent imaging has been demonstrated very effectively for *in vitro* imaging, the integrated fluorescent nanoprobes with other imaging modilities are generally necessary to overcome the drawbacks of fluorescent imaging *in vivo*.[259-263] As compared with single model imaging, the multimodel imaging using different output signals such as single photon emission computing tomography, magnetic resonances imaging, and positron emission tomography possess obvious advantages for *in vivo* biological imaging.[264] Liu et al have recently reported fluorescent-magnetic dual-modality AIE dots for *in vivo* tumor cell metastasis studies.[265] In this work, the AIE dots with surface amine and maleimide groups were fabricated through a nanoprecipitation strategy using 1,2-Distearoyl-sn-glycero-3-phosphoethanolamine-N-[amino(polyethylene glycol)-2000] (DSPE-PEG2000-NH2) and 1,2-distearoyl-sn-glycero-3-phosphoethanolamine-N-[maleimide(polyethylene glycol)-2000] (DSPE-PEG2000-Mal) as the surface coating compounds to encapsulate the AIE dye (TPEPAFN). And then the MR contrast (DTPA dianhydride) was conjugated with the surface amine groups for chelation of Gd(III). Finally, the targeting agent (Tat) through conjugation between maleimide groups on the dot surface and thiol groups at C-terminus of Tat peptide. The performance of Tat-Gd-AIE dots for cell labelling was examined using C6 glioma cells and the fluorescence images were recorded by confocal imaging. As compared with the Gd-AIE dot treated cells, much stronger fluorescence signal was observed in Tat-Gd-AIE dots, implying the Tat play a crucial role in improving living cell internalization efficiency of the Tat functionalized nanoprobes. The *in vivo* imaging of Tat-Gd-AIE dots in mice suggested that these dual model dots were mainly accumulated in the lung because of the pulmonary microvascular barrier. Due to the relative low sensitivity of MRI and the insufficient amount of Gd(III) in the injected cells, the dual model nanoprobes can not be detected through MRI upon intravenous injection into the mice though the Tat-Gd-AIE dots have been proven to be an efficient T1 contrast reagent with desired longitudinal relaxation time (**Fig. 16**). However, the incorporation of Gd(III) on dual-modality imaging dots is also very useful because the Gd allows accurate quantification of the biodistribution of injected cancer cells. Therefore, optimization of the AIE dot formulation is highly desirable if we tried to realize the *in vivo* cell tracking through MRI.

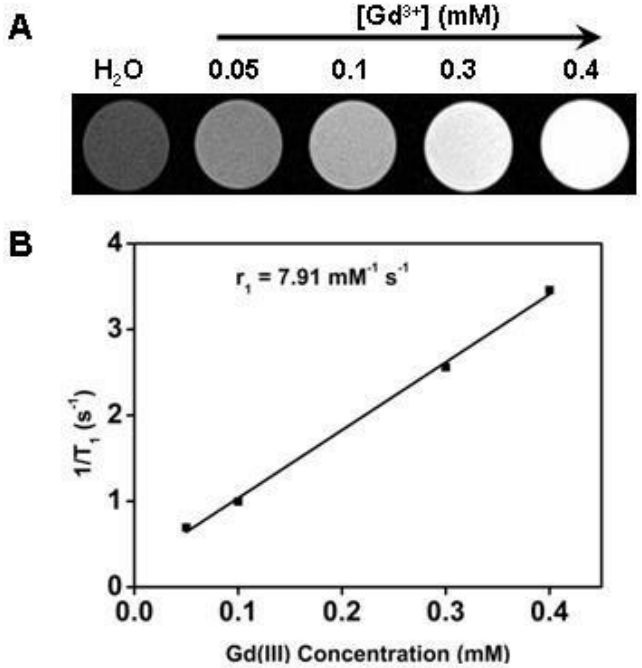

Fig. 16 (A) T1-weighted MR images of Tat-Gd-AIE dots at various Gd(III) concentrations of 0, 0.05, 0.1, 0.3, and 0.4 × 10−3 m. (B) Plot of water proton longitudinal relaxation rate (1/T1) of Tat-Gd-AIE dots as a function of Gd(III) concentration. (Reprinted with permission from Ref. [265]).

3.2 Biological Sensor

AIE dyes, which are non-emissive when molecularly dissolved but are induced to emit efficiently upon aggregation, have become very attractive for the design of novel fluorescent probes. After stimuli responsive components were contained in the AIE dye based nanoprobes, the biological sensor based on these novel nanoprobes can be constructed.[121, 122, 242, 266-284] For example, Chen et al simply conjugated tyrosine phosphate, a substrate for alkaline phosphatase (ALP), with the tetraphenylethylene fluorogen to generate the amphiphilic molecule 1, which exhibited excellent solubility in water at pH 7.4 due to the presence of two phosphate groups in its molecular structure. After the dephosphorylation reaction catalyzed by ALP, 1 was converted to 2, a relative more hydrophobic entity, resulting in the aggregation of AIE residues in aqueous solutions and the enhancement of the fluorescence signals.[285] The applicability of probe 1 was evaluated for studying endogenous ALP activities in living cells with HeLa cells (human cervical carcinoma cell line) and L-929 cells (mouse fibroblast cell line). The confocal fluorescence microscopy image of L-929 cells treated with 50 mM of 1 did not show obvious fluorescence signals inside the cells after 24 h incubation. However, in the case of ALP-positive HeLa cells, strong blue fluorescence was observed from a confocal microscopy image under the same conditions, suggesting the high-level expression of ALP inside the HeLa cell, which promoted the enzymatic dephosphorylation of 1 and lighted up the probe (**Fig. 17**).

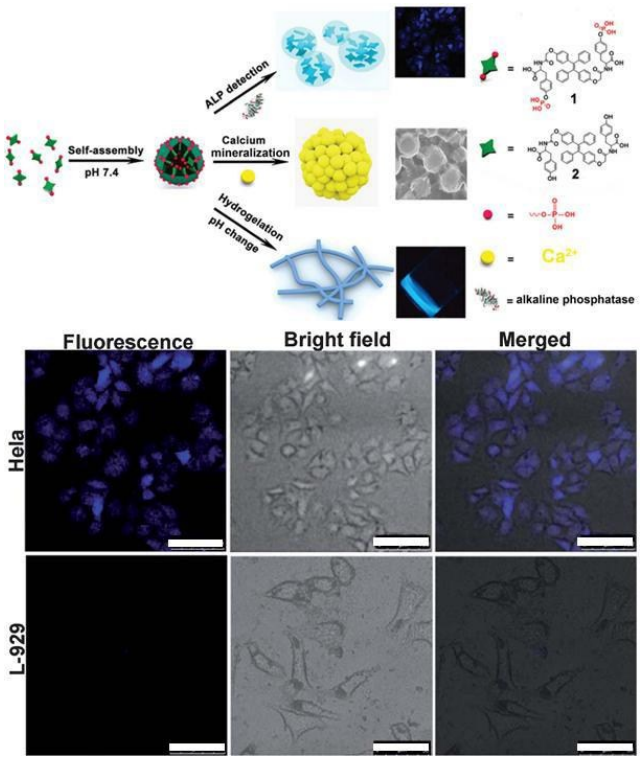

Fig. 17 Illustration of the multifunctionality of the tetraphenylethylene and tyrosine phosphate conjugate for fluorometric detection of alkaline phosphatase, supramolecular hydrogelation and biomimetic calcium mineralization (above); Fluorescence microscopy images of HeLa cells and L-929 cells incubated with probe 1 for ALP imaging (below). All images share the same scale bar (100 μm). (Reprinted with permission from ref. [285]).

Moreover, by incorporation of different chemical and biochemical functional groups into AIE dyes would lead to the generation of numerous molecules with unprecedented properties for biological sensing. A water-soluble fluorescent light-up bioprobe based on luminogen with AIE characteristics was developed by Liu et al for targeted intracellular thiol imaging.[239] They designed an integrin $\alpha_v\beta_3$ targeted light-up probe, which is composed of a targeted cyclic RGD (cRGD) peptide, a highly water soluble peptide with five aspartic acids (Asp, D5), a tetraphenylethene (TPE) fluorogen and a thiol-specific cleavable disulfide linker. cRGD exhibits high binding affinity towards $\alpha_v\beta_3$ integrin which is a unique molecular biomarker for early detection and treatment of rapidly growing solid tumors. The probe (TPE-SS-D5-cRGD) is highly water soluble and is almost non-fluorescent in aqueous media. The cleavage of the disulfide group by thiols leads to enhanced fluorescence signal output (**Fig. 18**). This probe has the potential for real-time monitoring of thiol levels in specific tumor cells (**Fig. 19**).

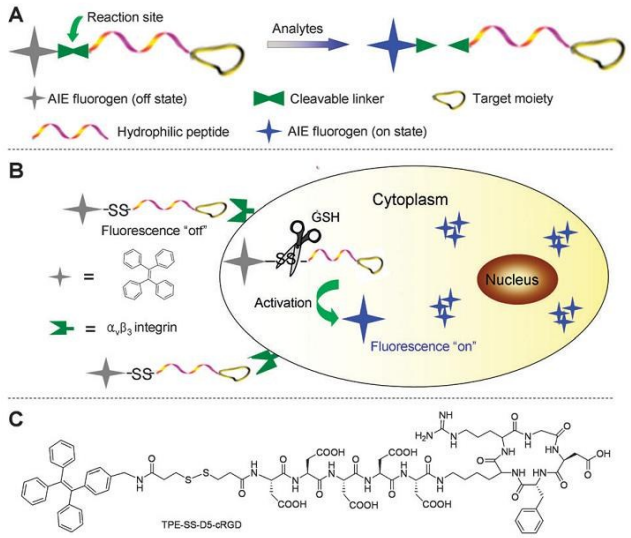

Fig. 18 (A) General probe design strategy and (B) schematic illustration of cRGD targeted imaging of intracellular thiols through $\alpha_v\beta_3$ integrin mediated cellular uptake and cleavage of the disulfide bond to induce fluorescence ''turn on''. (C) Chemical structure of the probe. (Reprinted with permission from ref. [239]).

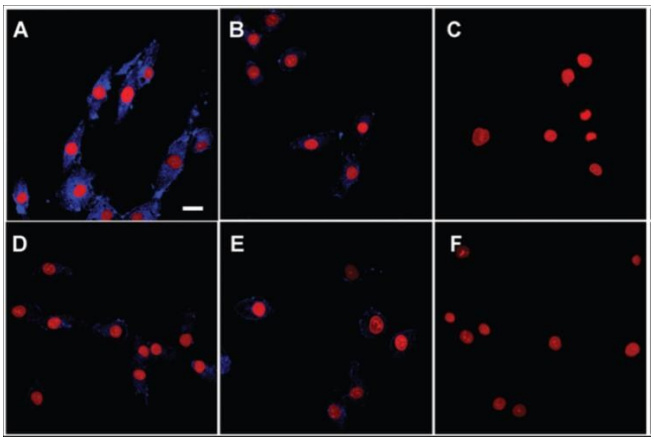

Fig. 19 Confocal microscopy images of U87-MG (A–C) and MCF-7 (D–F) cells after incubation with TPE-SS-D5-cRGD (A, D), TPE-SS-D5 (B, E) and TPE-CC-D5 (C, F). The nuclei were stained with propidium iodide. All images share the same scale bar (20 μm). (Reprinted with permission from ref. [239]).

Interestingly, bioprobes based on AIE dyes with stereoisomers could also be developed for biological significant targets, which may not only aid in stereochemistry studies, but also shed light on the mechanism of ligand–target interaction for a wide range of clinical and diagnostic applications.[286] A dual-labeled probe for monitoring caspase activity was designed and synthesized based on a TPE fluorogen with AIE characteristics and a caspase specific Asp-Glu-Val-Asp (DEVD) peptide by Liu's group (**Fig. 20**). Two stereoisomers were furnished and successfully separated by HPLC. They demonstrated for the first time the effect of isomerization on the reaction kinetics between the probes and caspase. It was revealed that caspase can produce a much higher light-up ratio for the Z-TPE-2DEVD probe, while its kinetics favor E-TPE-2DEVD due to enhanced probability of optimal binding between the two. Understanding the stereoisomers and their biological functions will open new opportunities for bioprobe design with optimized performance (**Fig. 21**).

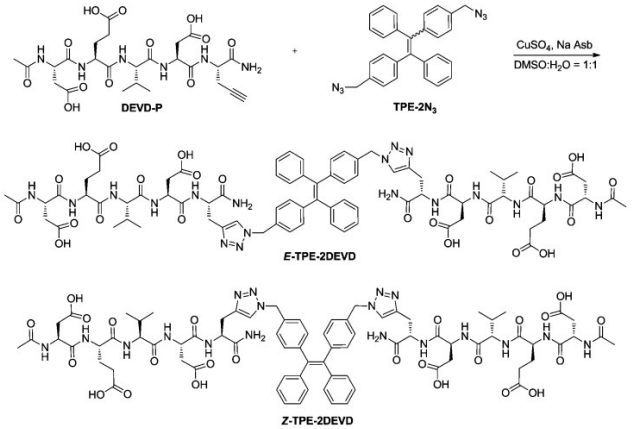

Fig. 20 "Click" synthesis of E- and Z-TPE-2DEVD. (Reprinted with permission from ref. [286]).

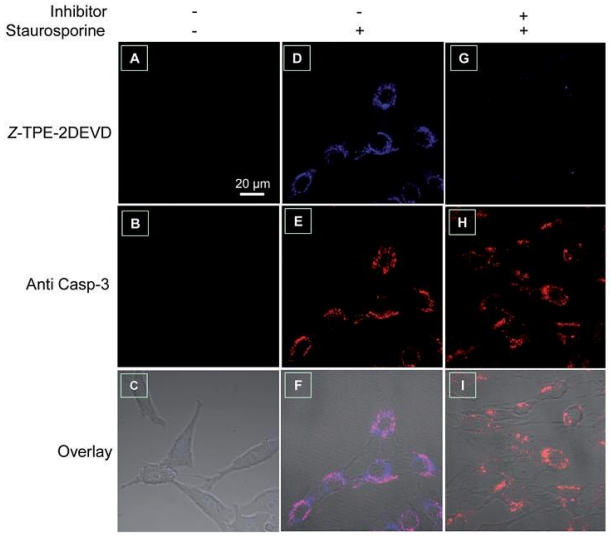

Fig. 21 CLSM images of normal MCF-7 cells treated with Z-TPE-2DEVD (A–C); apoptotic MCF-7 cells treated with Z-TPE-2DEVD (D–F), apoptotic MCF-7 cells treated with Z-TPE-2DEVD, inhibitor (10 μM), and caspase-3 antibody (G–I). Staurosporine (STS, 1 μM) was used to induce cell apoptosis. Blue: probe fluorescence; red: immunofluorescence signal generated from an anti-caspase-3 primary antibody and a Texas Red-labeled secondary antibody. The signals were collected using DAPI and Texas Red filters for blue and red emissions, respectively. All images share the same scale bar (20 μm). (Reprinted with permission from ref. [286]).

3.3 Theranostics

Various nanoparticles have been employed for targeted drug delivery. However, the sole role of these traditional nanoparticles is to deliver drugs into cancer cells. To date, targeted drug delivery to tumor cells with minimized side effects and real-time in situ monitoring of drug efficacy is highly desirable for personalized medicine. Therefore, fluorescent nanoparticles functionalized with targeted drugs based on AIE dyes have great potential in this area due to their special fluorescence properties.[287-295]

Liu et al designed and synthesized an asymmetric fluorescent light-up bioprobe with AIE characteristics by the conjugation of two different hydrophilic peptides, caspase-specific Asp-Glu-Val-Asp (DEVD) and cyclic Arg-Gly-Asp (cRGD), onto a typical AIE luminogen of a tetraphenylsilole (TPS) unit.[296] By virtue of the specific binding between cRGD peptide and integrin $\alpha_v\beta_3$ receptors, the Ac-DEVD-TPS-cRGD should be favorably internalized by integrin $\alpha_v\beta_3$ receptor-overexpressed cancer cells over other cells with low receptor expression on the cell membrane. The asymmetric probe is almost non-emissive in aqueous solution and its fluorescence is significantly switched on in the presence of caspase-3. The fluorescence turn-on is due to the cleavage of the DEVD moiety by caspase-3, and the aggregation of released TPS-cRGD residues, which restricts the intramolecular rotations of TPS phenyl rings and populates the radiative decay channels (**Fig. 22**). Application of the asymmetric light-up probe for real-time targeted imaging of cancer cell apoptosis is successfully demonstrated using integrin $\alpha_v\beta_3$ receptor overexpressing U87MG human glioblastoma cells as an example. The probe shows specific targeting capability to U87MG cancer cells by virtue of the efficient binding between cRGD and integrin $\alpha_v\beta_3$ receptors and is able to real-time monitor and image cancer cell apoptosis in a specific and sensitive manner (**Fig. 23**).

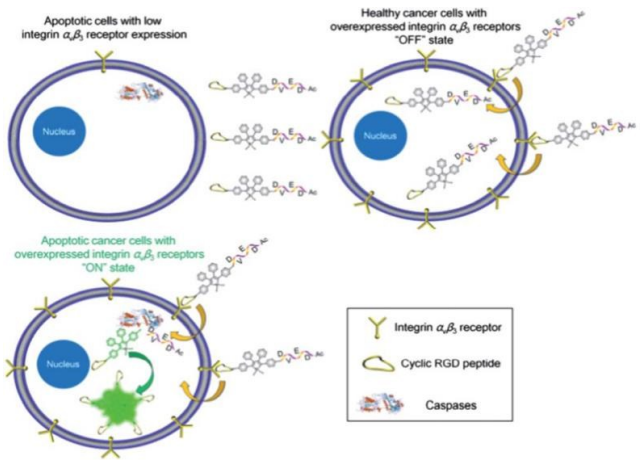

Fig. 22 The principle of apoptosis imaging in target cancer cell based on Ac-DEVD-TPS-cRGD. (Reprinted with permission from ref. [296]).

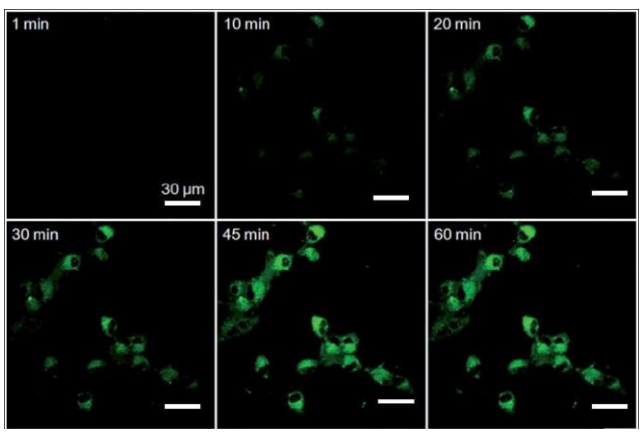

Fig. 23 Real-time CLSM images displaying the apoptotic progress of Ac-DEVD-TPS-cRGD-stained U87MG cells upon STS induced apoptosis at room temperature. [Ac-DEVD-TPS-cRGD] = 5 μM, [STS] = 1 μM. All images share the same scale bar (30 μm). (Reprinted with permission from ref. [296]).

In order to further evaluation their applications in targeted drug delivery, Liu et al synthesized a chemotherapeutic Pt (IV) prodrug whose two axial positions are functionalized with cRGD tripeptide for targeting integrin $\alpha_v\beta_3$ overexpressed cancer cells and an apoptosis sensor which is composed of TPS fluorophore with AIE characteristics and a caspase-3 enzyme specific DEVD peptide.[297] The targeted Pt(IV) prodrug can selectively bind to $\alpha_v\beta_3$ integrin overexpressed cancer cells to facilitate cellular uptake. In addition, the Pt(IV) prodrug can be reduced to active Pt(II) drug in cells and release the apoptosis sensor TPS-DEVD simultaneously. The reduced Pt(II) drug can induce the cell apoptosis and activate caspase-3 enzyme to cleave the DEVD peptide sequence. Due to free rotation of the phenylene rings, TPS-DEVD is nonemissive in aqueous media. The specific cleavage of DEVD by caspase-3 generates the hydrophobic TPS residue, which tends to aggregate, resulting in restriction of intramolecular rotations of the phenyl rings and ultimately leading to fluorescence enhancement (**Fig. 24**). Such noninvasive and real-time imaging of drug-induced apoptosis in situ can be used as an indicator for early evaluation of the therapeutic responses of a specific anticancer drug (**Fig. 25**).

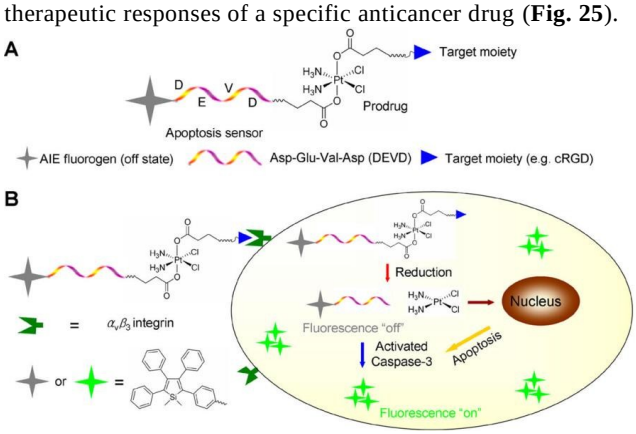

Fig. 24 Schematic illustration of the targeted theranostic Platinum(IV) prodrug with a built-in aggregation-induced emission (AIE) light-up apoptosis sensor for noninvasive in situ early evaluation of its therapeutic responses. (Reprinted with permission from ref. [297]).

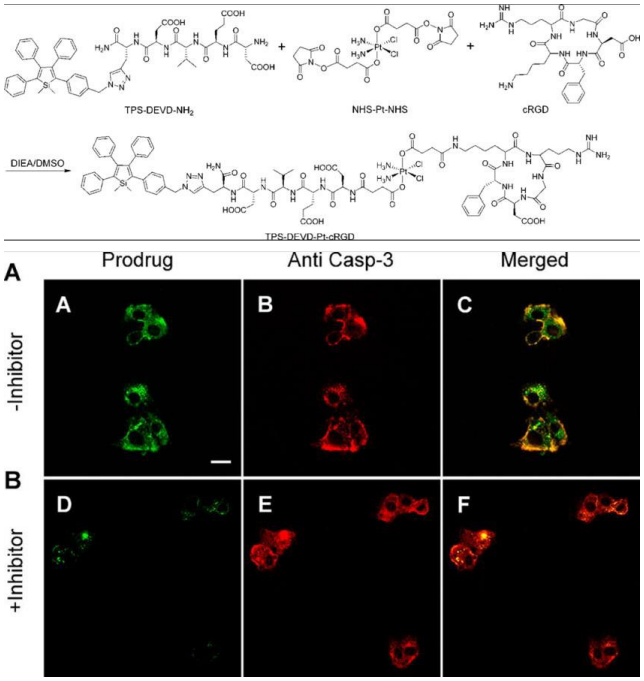

Fig. 25 Synthetic route to the theranostic prodrug of TPS-DEVD-Pt-cRGD (above); CLSM images of U87-MG cells upon treatment with TPS-DEVD-Pt-cRGD (5μM) and caspase-3 antibody (A−C) or TPS-DEVD-Pt-cRGD (5 μM) in the presence of inhibitor 5-[(S)-(+)-2-(methoxymethyl)pyrrolidino] sulfonylisatin (5 μM) and caspase-3 antibody (D−F). Green = probe fluorescence; red = immunofluorescence signal generated from anti-caspase-3 primary antibody and a Texas Red-labeled secondary antibody. All images share the same scale bar (20 μm). (Reprinted with permission from ref. [297]).

Liang et al developed a drug delivery system using tetraphenylethene (TPE) to fabricate a self-assembly micelle with AIE properties.[286] AIE makes the nanocarriers visible for high-quality imaging and the switching on and off of the AIE is intrinsically controlled by the assembly and disassembly of the micelles. This DDS was tested for doxorubicin (DOX) delivery and intracellular imaging. The fluorescence intensity of both TPE and DOX decreased upon forming TPE micelles loaded with DOX (TPED) due to fluorescence resonance energy transfer (FRET) because of the overlap between the emission of TPE and the absorption of DOX. After DOX leaked out of TPED, the fluorescence of the DOX would increase because it is no longer quenched by ACQ effect and the fluorescence of the TPE would increase because the emission from TPE is no longer transferred by FRET to DOX (**Fig. 26**). For TPED, the DOX content reached as much as 15.3% by weight, and the anticancer efficiency was higher than for free DOX. Meanwhile, high-quality imaging was obtained to trace the intracellular delivery of the TPED (**Fig. 27**).

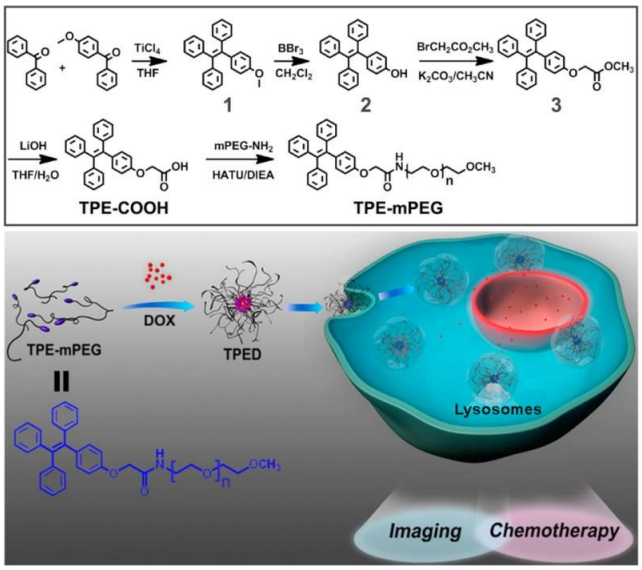

Fig. 26 Synthetic route of TPE−mPEG and schematic illustration of DOX-loaded self-assembly micelle (TPED) with AIE as a novel multifunctional theranostic platform for intracellular imaging and cancer treatment. (Reprinted with permission from ref. [286]).

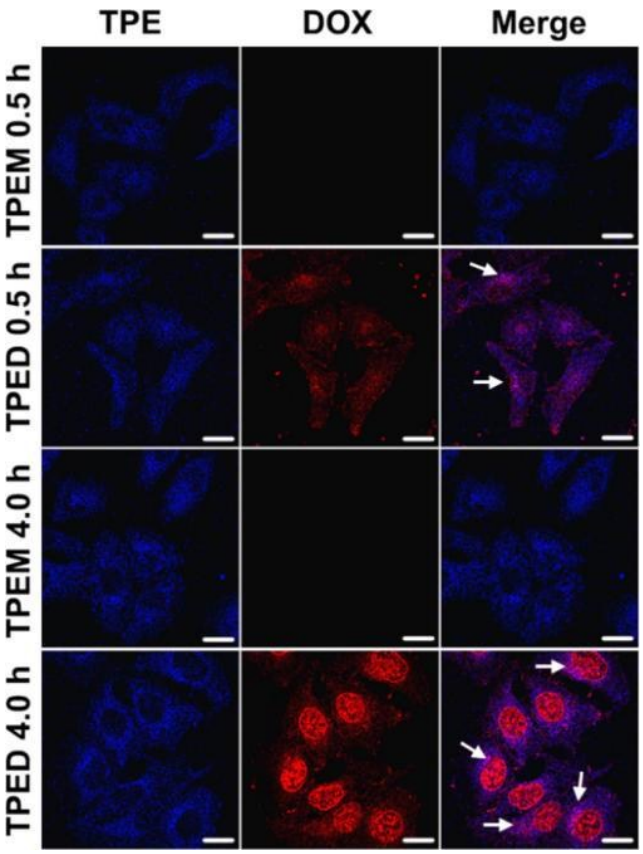

Fig. 27 Spatial distributions of TPEM and TPED in MCF-7 cells. CLSM images of the distribution of self-indicating TPEM and TPED. MCF-7 breast cancer cells were incubated with TPEM (75 μM) and TPED (TPE−mPEG 75 μM and DOX 5.0 μM) for 0.5 and 4 h. Scale bars are 20 μm. (Reprinted with permission from ref. [286]).

A self-indicating drug delivery system (SIDDS) has also been developed by Liang's group, which is capable of revealing spatiotemporal drug release.[298] TPE assembled to self-luminescent nanoparticles, which showed AIE and can

easily be tracked in cells. TPE NPs displayed no cytotoxicity and did not enter the nucleus, the function implementation site of the drugs (DOX). Then, antitumor drug DOX was bonded to TPE NPs via electrostatic interaction and formed a new drug delivery system (TD NPs) (**Fig. 28**). As designed, drug releasing was pH-sensitive, DOX detached from TD NPs only in organelles with a low internal pH, like lysosomes. In fluorescence microscope image, TD NPs, TPE NPs and free DOX showed three different "colors", by observing the transition of those "colors", the sub-cellular location of TPE NPs and free DOX can be determined, and also, the drug releasing site of TD NPs was indicated. Furthermore, the SIDDS were more effective in inhibiting the proliferation of cancer cells (**Fig. 29**).

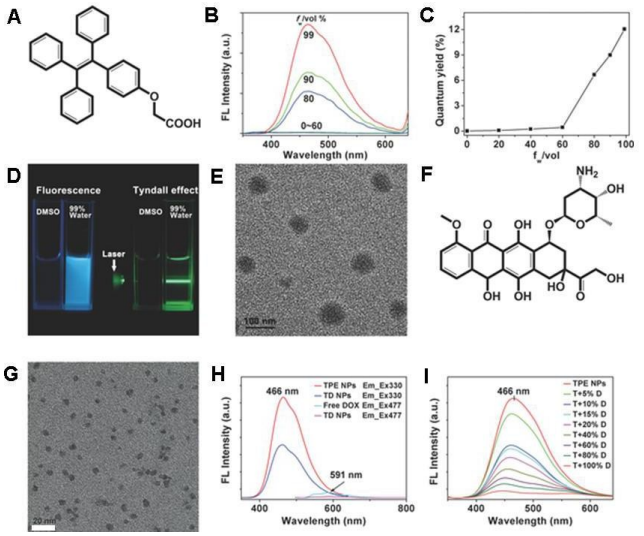

Fig. 28 Fluorescent behaviors and nano-aggregates of TPE aggregates and TPE/DOX complex nanoparticles. A) Chemical structure of carboxylated TPE (TPE-COOH). B) FL spectra of TPE (50 μM) in DMSO/water mixtures with different fractions of water (f_w). C) The change of the quantum yields (Φ_F) of TPE-COOH with the increment of water fraction in the DMSO/water mixture. The Φ_F values were estimated using quinine sulfate in 0.1 N H_2SO_4 (Φ_F = 54.6%) as standard. D) Fluorescence and Tyndall effect of TPE solutions. E) TEM image of TPE nano-aggregates (50 μM). f) Chemical structures of doxorubicin (DOX). G) TEM image of nanoaggregates of TPE (50 μM) and 10% DOX (5 μM) formed in a DMSO/water mixture with f_w = 99.9 vol%, the scale bar of image (20 nm). H) FL spectra of TPE NPs (50 μM), TD NPs (50 μM TPE and 5 μM DOX), and free DOX (5 μM). TPE λ_{ex} = 330 nm; DOX λ_{ex} = 477 nm. I) Fluorescence changes of TPE when adding different molar ratios of DOX (5% ~100%). TPE λ_{ex} = 330 nm. (Reprinted with permission from ref. [298]).

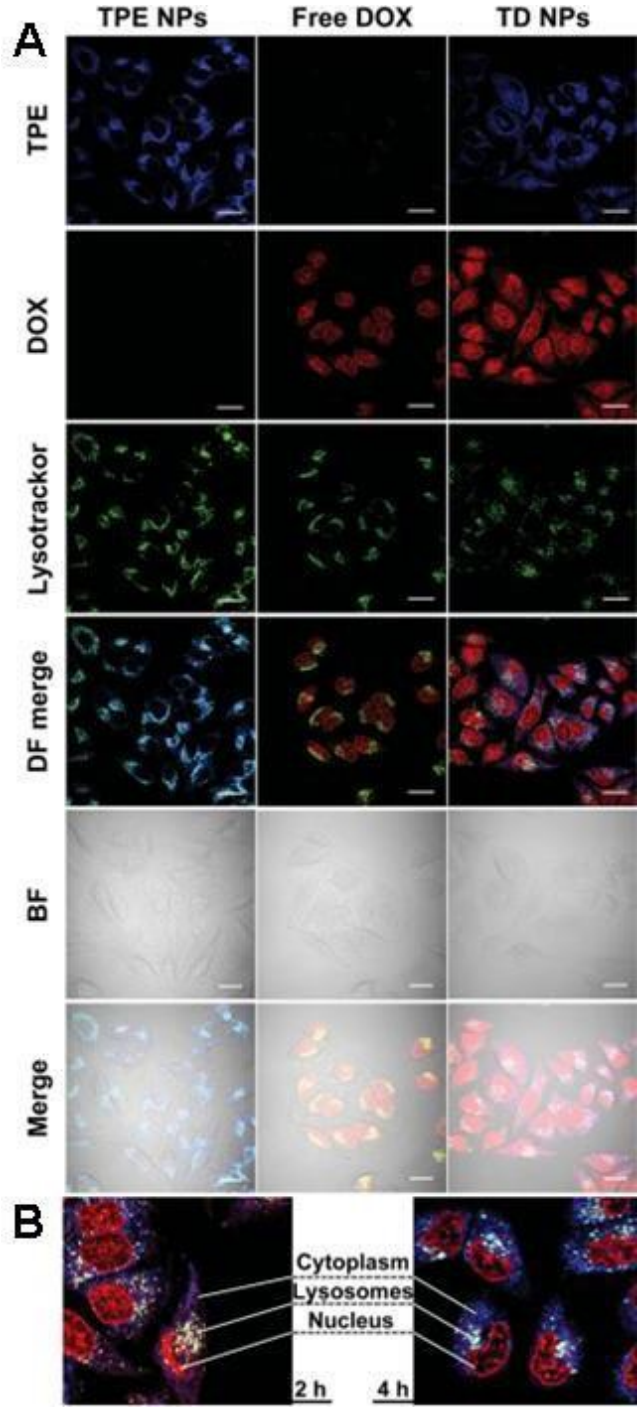

Fig. 29 Spatial distributions of TPE NPs, DOX and TD NPs in MCF-7s cells. A) CLSM images of elf-indicating TPE NPs, DOX and TD NPs distribution, and lysosomes, indicated by Lysotracker Green. The breast cancer MCF-7s cells were incubating with TPE NPs (40 μM), DOX (4 μM) and TD NPs (40 μM) for 2 h. Scale bars are 30 μm. B) Detailed TD NPs spatiotemporal distributions in MCF-7s cells. (Reprinted with permission from ref. [298]).

Wei et al have recently developed the one-pot preparation of fluorescent mesoporous silica nanoparticles (MSNs) using an AIE material An18 (derivative from 9,10-distyrylanthracene with alkoxyl end group) as fluorogen and a cationic surfactant cetyltrimethyl ammonium bromide (CTAB) as structure-directed template and cell killer agent.[299]

As shown in **Fig. 30**, An18 and CTAB were first dispersed in THF and H_2O. The AIE dye containing micelles (An18-CTAB) could be easily formed with the increase of the water content in solution. The An18-CTAB could further serve as the structure direct template for preparation of MSNs. After removal of THF from the reaction systems, An18-CTAB was encapsulated in MSNs, thus making MSNs luminescent (**Fig. 30**). These fluorescent MSNs demonstrated good biocompatibility and can be used for cell imaging. The anticancer effectiveness of AIE MSNs to A549 cells was also determined. On the other hand, the CTAB is a renown anticancer agent. Therefore, the anticancer effect of these luminescent silica nanoparticles contained CTAB (AIE-MSNs-1) was evaluated. Results suggested that these AIE-MSNs-1 exhibited obviously cytotoxicity toward A549 cells, indicating that AIE-MSNs-1 is promising for nanotheranostic applications.

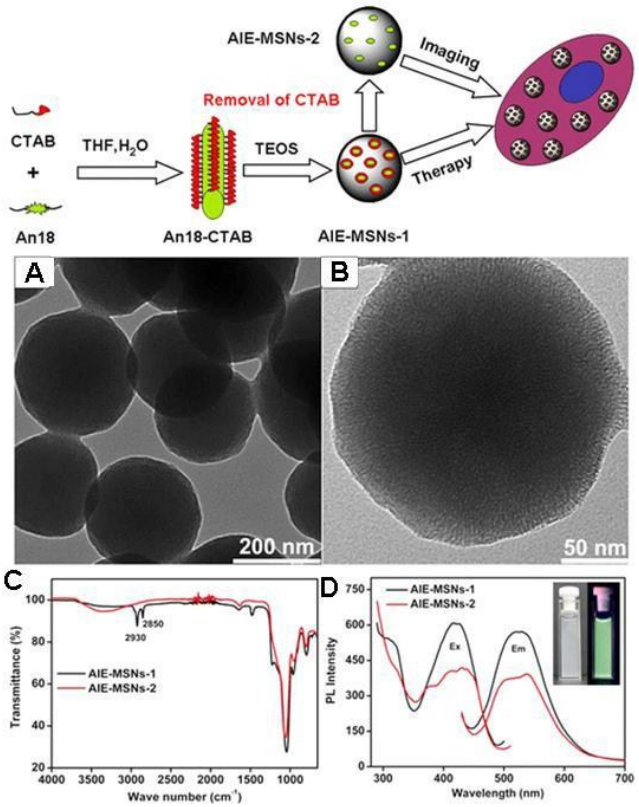

Fig. 30 Schematic showing the Preparation of AIE-MSNs and Their Utilized for Cell Imaging and Cancer Therapy Applications (above); Characterization of AIE-MSNs. (A, B) TEM images of AIE MSNs-1. (C) FT-IR spectra of AIE-MSNs-1 and AIE-MSNs-2, (D) excitation and emission (excited by wavelength of 405 nm) spectra of AIE-MSNs-1 and AIE-MSNs-2, the insets are images of AIE-MSNs-2 dispersed in water (left) and excited by UV lamp (λ= 365 nm, right). (Reprinted with permission from ref. [299]).

4. Conclusion

AIE dye based polymeric nanoparticles are recently emerged luminescent nanoprobes, that combination of the unique properties of AIE dyes and polymers. A number of strategies such as noncovalent self assembly of AIE dyes and amphiphilic molecules, covalent conjugation of AIE dyes with hydrophilic molecules, polymerization of AIE dyes with other monomers and encapsulation of AIE dyes in silica nanoparticles etc for fabrication of these AIE dye based nanoprobes have been summarized in this review. The biomedical applications such as biological imaging, biological sensor and theranostics of these AIE nanosystems were also highlighted. However, the biomedical applications of AIE dye based nanoprobes are mainly focused on biological imaging, the biological sensor and nanotheranostic systems of these nanoprobes are only in their infancy state. On the other hand, due to the high fluroescence background of biological systems, the biological imaging only using fluorescence signal will not fulfill the requirements for mordern biomedical applications. Therefore, design novel AIE dyes with better fluorescent properties and extended the biomedical applications of the AIE nanoprobes may be the future direction of this field. Finally, although much effort has been devoted toward the fabrication and biomedical applications of polymeric AIE dye based nanoprobes, most of current studies have focused on the *in vitro* biomedical applications of AIE dye based nanomaterials. More work for their *in vivo* biomedical applications as well as biological behaviors including adsorption, distribution, metabolism and excretion is required. Furthermore, detailed information about long term toxicity of AIE dye based polymeric nanoprobes should be provided in future.

Acknowledgements

This research was supported by the National Science Foundation of China (Nos. 21134004, 21201108, 51363016, 21474057), and the National 973 Project (Nos. 2011CB935700).

Notes

[a] Department of Chemistry, Nanchang University, 999 Xuefu Avenue, Nanchang 330031, China. [b] Department of Chemistry and the Tsinghua Center for Frontier Polymer Research, Tsinghua University, Beijing, 100084, P. R. China.
Xiaoyongzhang@1980@gmail.com , weiyen@tsinghua.edu.cn

References

1. V. Wagner, A. Dullaart, A.-K. Bock and A. Zweck, *Nat. Biotechnol.*, 2006, **24**, 1211-1217.
2. H. Xu, Q. Li, L. Wang, Y. He, J. Shi, B. Tang and C. Fan, *Chem. Soc. Rev.*, 2014, **43**, 2650-2661.
3. Y. Liu, D. Tu, H. Zhu and X. Chen, *Chem. Soc. Rev.*, 2013, **42**, 6924-6958.
4. M. Montalti, L. Prodi, E. Rampazzo and N. Zaccheroni, *Chem. Soc. Rev.*, 2014, **43**, 4243-4268.
5. R. Hu, N. L. Leung and B. Z. Tang, *Chem. Soc. Rev.*, 2014, **43**, 4494-4562.
6. W. C. Chan and S. Nie, *Science*, 1998, **281**, 2016-2018.
7. M. Chen and M. Yin, *Prog. Polym. Sci.*, 2014, **39**, 365-395.
8. J. Yao, M. Yang and Y. Duan, *Chem. Rev.*, 2014, **114**, 6130-6178.
9. W. Kong, J. Liu, R. Liu, H. Li, Y. Liu, H. Huang, K. Li, J. Liu, S.-T. Lee and Z. Kang, *Nanoscale*, 2014, **6**, 5116-5120.
10. Y. He, Y. Zhong, F. Peng, X. Wei, Y. Su, Y. Lu, S. Su, W. Gu, L. Liao and S.-T. Lee, *J. Am. Chem. Soc.*, 2011, **133**, 14192-14195.
11. Z. Ding, B. M. Quinn, S. K. Haram, L. E. Pell, B. A. Korgel and A. J. Bard, *Science*, 2002, **296**, 1293-1297.

12. L. Li, G. Wu, G. Yang, J. Peng, J. Zhao and J.-J. Zhu, *Nanoscale*, 2013, **5**, 4015-4039.
13. D.-E. Lee, H. Koo, I.-C. Sun, J. H. Ryu, K. Kim and I. C. Kwon, *Chem. Soc. Rev.*, 2012, **41**, 2656-2672.
14. T. L. Doane and C. Burda, *Chem. Soc. Rev.*, 2012, **41**, 2885-2911.
15. R. Mout, D. F. Moyano, S. Rana and V. M. Rotello, *Chem. Soc. Rev.*, 2012, **41**, 2539-2544.
16. X. Zhang, S. Wang, M. Liu, B. Yang, L. Feng, Y. Ji, L. Tao and Y. Wei, *Phys. Chem. Chem. Phys.*, 2013, **15**, 19013-19018.
17. V. Brunetti, H. Chibli, R. Fiammengo, A. Galeone, M. A. Malvindi, G. Vecchio, R. Cingolani, J. L. Nadeau and P. P. Pompa, *Nanoscale*, 2013, **5**, 307-317.
18. H. Sugimoto, M. Fujii, Y. Fukuda, K. Imakita and K. Akamatsu, *Nanoscale*, 2014, **6**, 122-126.
19. R. Jin, *Nanoscale*, 2010, **2**, 343-362.
20. Y. Xu, J. Sherwood, Y. Qin, D. Crowley, M. Bonizzoni and Y. Bao, *Nanoscale*, 2014, **6**, 1515-1524.
21. S. Raut, R. Rich, R. Fudala, S. Butler, R. Kokate, Z. Gryczynski, R. Luchowski and I. Gryczynski, *Nanoscale*, 2014, **6**, 385-391.
22. C. V. Conroy, J. Jiang, C. Zhang, T. Ahuja, Z. Tang, C. A. Prickett, J. J. Yang and G. Wang, *Nanoscale*, 2014, **6**, 7416-7423.
23. J. Hou, J. Yan, Q. Zhao, Y. Li, H. Ding and L. Ding, *Nanoscale*, 2013, **5**, 9558-9561.
24. S. Zhu, Q. Meng, L. Wang, J. Zhang, Y. Song, H. Jin, K. Zhang, H. Sun, H. Wang and B. Yang, *Angew. Chem. Int. Ed.*, 2013, **125**, 4045-4049.
25. S. Zhu, J. Zhang, X. Liu, B. Li, X. Wang, S. Tang, Q. Meng, Y. Li, C. Shi and R. Hu, *RSC Adv.*, 2012, **2**, 2717-2720.
26. Y. Song, S. Zhu and B. Yang, *RSC Adv.*, 2014, **4**, 27184-27200.
27. S. Liu, J. Tian, L. Wang, Y. Zhang, X. Qin, Y. Luo, A. M. Asiri, A. O. Al-Youbi and X. Sun, *Adv. Mater.*, 2012, **24**, 2037-2041.
28. Y.-P. Sun, B. Zhou, Y. Lin, W. Wang, K. S. Fernando, P. Pathak, M. J. Meziani, B. A. Harruff, X. Wang and H. Wang, *J. Am. Chem. Soc.*, 2006, **128**, 7756-7757.
29. J. Xie, Y. Zheng and J. Y. Ying, *J. Am. Chem. Soc.*, 2009, **131**, 888-889.
30. K. Wang, X. Yuan, Z. Guo, J. Xu and Y. Chen, *Carbohyd. polym.*, 2014, **102**, 699-707.
31. G. Leménager, E. De Luca, Y.-P. Sun and P. P. Pompa, *Nanoscale*, 2014, **6**, 8617-8623.
32. X. Zhang, S. Wang, C. Zhu, M. Liu, Y. Ji, L. Feng, L. Tao and Y. Wei, *J. Colloid Interf. Sci.*, 2011, **397**, 39-44.
33. Y.-P. Guo, T. Long, S. Tang, Y.-J. Guo and Z.-A. Zhu, *J. Mater. Chem. B*, 2014, **2**, 2899-2909.
34. D. S. Morais, J. Coelho, M. P. Ferraz, P. S. Gomes, M. H. Fernandes, N. S. Hussain, J. D. Santos and M. A. Lopes, *J. Mater. Chem. B*, 2014, **2**, 5872-5881.
35. Z. Chen, H. Chen, H. Hu, M. Yu, F. Li, Q. Zhang, Z. Zhou, T. Yi and C. Huang, *J. Am. Chem. Soc.*, 2008, **130**, 3023-3029.
36. J. Zhou, Z. Liu and F. Li, *Chem. Soc. Rev.*, 2012, **41**, 1323-1349.
37. Y. Yang, Q. Zhao, W. Feng and F. Li, *Chem. Rev.*, 2012, **113**, 192-270.
38. X. Teng, Y. Zhu, W. Wei, S. Wang, J. Huang, R. Naccache, W. Hu, A. I. Y. Tok, Y. Han and Q. Zhang, *J. Am. Chem. Soc.*, 2012, **134**, 8340-8343.
39. O. S. Wolfbeis, *Chem. Soc. Rev.*, 2015, 10.1039/C1034CS00392F.
40. C. Yu, X. Li, F. Zeng, F. Zheng and S. Wu, *Chem. Commun.*, 2013, **49**, 403-405.
41. J. Hui, X. Zhang, Z. Zhang, S. Wang, L. Tao, Y. Wei and X. Wang, *Nanoscale*, 2012, **4**, 6967-6970.
42. X. Zhang, J. Hui, B. Yang, Y. Yang, D. Fan, M. Liu, L. Tao and Y. Wei, *Polym. Chem.*, 2013, **4**, 4120-4125.
43. N. Chen, Y. He, Y. Su, X. Li, Q. Huang, H. Wang, X. Zhang, R. Tai and C. Fan, *Biomaterials*, 2012, **33**, 1238-1244.
44. Y.-C. Yeh, K. Saha, B. Yan, O. R. Miranda, X. Yu and V. M. Rotello, *Nanoscale*, 2013, **5**, 12140-12143.
45. S. You, Q. Cai, K. Müllen, W. Yang and M. Yin, *Chem. Commun.*, 2014, **50**, 823-825.
46. K. Li and B. Liu, *Chem. Soc. Rev.*, 2014, **43**, 6570-6597.
47. H.-S. Peng and D. T. Chiu, *Chem. Soc. Rev.*, 2015, 10.1039/C1034CS00294F
48. X. Zhang, S. Wang, L. Xu, L. Feng, Y. Ji, L. Tao, S. Li and Y. Wei, *Nanoscale*, 2012, **4**, 5581-5584.
49. D. Ding, K. Li, Z. Zhu, K.-Y. Pu, Y. Hu, X. Jiang and B. Liu, *Nanoscale*, 2011, **3**, 1997-2002.
50. J. Geng, J. Liu, J. Liang, H. Shi and B. Liu, *Nanoscale*, 2013, **5**, 8593-8601.
51. M. Kumar and S. J. George, *Nanoscale*, 2011, **3**, 2130-2133.
52. C. Zhu, L. Liu, Q. Yang, F. Lv and S. Wang, *Chem. Rev.*, 2012, **112**, 4687-4735.
53. J. Liu, J. Geng, L.-D. Liao, N. Thakor, X. Gao and B. Liu, *Polym. Chem.*, 2014, **5**, 2854-2862.
54. G. Wang, H. Yin, J. C. Y. Ng, L. Cai, J. Li, B. Z. Tang and B. Liu, *Polym. Chem.*, 2013, **4**, 5297-5304.
55. J. Liu, G. Feng, D. Ding and B. Liu, *Polym. Chem.*, 2013, **4**, 4326-4334.
56. L. Zhou, J. Geng, G. Wang, J. Liu and B. Liu, *Polym. Chem.*, 2013, **4**, 5243-5251.
57. Y. Qu, X. Zhang, Y. Wu, F. Li and J. Hua, *Polym. Chem.*, 2014, **5**, 3396-3403.
58. Z. Li, M. Zheng, X. Guan, Z. Xie, Y. Huang and X. Jing, *Nanoscale*, 2014, **6**, 5662-5665.
59. Q. Zhao, C. Huang and F. Li, *Chem. Soc. Rev.*, 2011, **40**, 2508-2524.
60. H. Shi, H. Sun, H. Yang, S. Liu, G. Jenkins, W. Feng, F. Li, Q. Zhao, B. Liu and W. Huang, *Adv. Funct. Mater.*, 2013, **23**, 3268-3276.
61. W. Hu, X. Lu, R. Jiang, Q. Fan, H. Zhao, W. Deng, L. Zhang, L. Huang and W. Huang, *Chem. Commun.*, 2013, **49**, 9012-9014.
62. Z. Yang, Y. Yuan, R. Jiang, N. Fu, X. Lu, C. Tian, W. Hu, Q. Fan and W. Huang, *Polym. Chem.*, 2014, **5**, 1372-1380.
63. B. Bao, N. Tao, D. Yang, L. Yuwen, L. Weng, Q. Fan, W. Huang and L. Wang, *Chem. Commun.*, 2013, **49**, 10623-10625.
64. X.-q. Zhang, X.-y. Zhang, B. Yang and Y. Wei, *Chinese J. Polym. Sci.*, 2014, **32**, 1479-1488.
65. X.-q. Zhang, X.-y. Zhang, B. Yang and Y. Wei, *Chinese J. Polym. Sci.*, 2014, **32**, 871-879.
66. Z. Xu, B. He, J. Shen, W. Yang and M. Yin, *Chem. Commun.*, 2013, **49**, 3646-3648.
67. D. Shen, F. Zhou, Z. Xu, B. He, M. Li, J. Shen, M. Yin and C. An, *J. Mater. Chem. B*, 2014, **2**, 4653-4659.
68. L. Jiang, L. Ding, B. He, J. Shen, Z. Xu, M. Yin and X. Zhang, *Nanoscale*, 2014, **6**, 9965-9969.
69. Z. Xu, B. He, W. Wei, K. Liu, M. Yin, W. Yang and J. Shen, *J. Mater. Chem. B*, 2014, **2**, 3079-3086.
70. J. Zhang, S. You, S. Yan, K. Müllen, W. Yang and M. Yin, *Chem. Commun.*, 2014, **50**, 7511-7513.
71. G. Wu, F. Zeng and S. Wu, *Anal. Methods*, 2013, **5**, 5589-5596.
72. X. Zhang, X. Zhang, B. Yang, J. Hui, M. Liu, Z. Chi, S. Liu, J. Xu and Y. Wei, *Polym. Chem.*, 2014, **5**, 318-322.
73. X. Zhang, X. Zhang, B. Yang, J. Hui, M. Liu, Z. Chi, S. Liu, J. Xu and Y. Wei, *J. Mater. Chem. C*, 2014, **2**, 816-820.
74. X. Zhang, X. Zhang, B. Yang, J. Hui, M. Liu and Y. Wei, *Colloids Surf. B Biointerfaces*, 2014, **116**, 739-744.
75. X. Zhang, X. Zhang, B. Yang, Y. Yang and Y. Wei, *Polym. Chem.*, 2014, **5**, 5885-5889.
76. M. Liu, X. Zhang, B. Yang, Z. Li, F. Deng, Y. Yang, X. Zhang and Y. Wei, *Carbohyd. Polym.*, 2015, **121**, 49-55.
77. X. Zhang, X. Zhang, B. Yang, Y. Yang, Q. Chen and Y. Wei, *Colloids Surf. B Biointerfaces*, 2014, **123**, 747-752.
78. K. Wang, X. Zhang, X. Zhang, B. Yang, Z. Li, Q. Zhang, Z. Huang and Y. Wei, *Colloids Surf. B Biointerfaces*, 2015, **126**, 273-279.
79. X. Zhang, M. Liu, B. Yang, X. Zhang and Y. Wei, *Colloids Surf. B Biointerfaces*, 2013, **112**, 81-86.
80. M. Liu, X. Zhang, B. Yang, F. Deng, J. Ji, Y. Yang, Z. Huang, X. Zhang and Y. Wei, *RSC Adv.*, 2014, **4**, 22294-22298.
81. H. Li, X. Zhang, X. Zhang, B. Yang, Y. Yang, Z. Huang and Y. Wei, *RSC Adv.*, 2014, **4**, 21588-21592.
82. X. Zhang, Z. Ma, M. Liu, X. Zhang, X. Jia and Y. Wei, *Tetrahedron*, 2013, **69**, 10552-10557.
83. N. Na, F. Wang, J. Huang, C. Niu, C. Yang, Z. Shang, F. Han and J. Ouyang, *RSC Adv.*, 2014, **4**, 35459-35462.
84. C. Li, W.-L. Gong, Z. Hu, M. P. Aldred, G.-F. Zhang, T. Chen, Z.-L. Huang and M.-Q. Zhu, *Tetrahedron*, 2013, **RSC Adv.**, 8967-8972.

85. B. Daglar, E. Ozgur, M. Corman, L. Uzun and G. Demirel, *RSC Adv.*, 2014, **4**, 48639-48659.
86. B. He, Y. Chu, M. Yin, K. Müllen, C. An and J. Shen, *Adv. Mater.*, 2013, **25**, 4580-4584.
87. M. Yin, J. Shen, G. O. Pflugfelder and K. Müllen, *J. Am. Chem. Soc.*, 2008, **130**, 7806-7807.
88. M. Yin, J. Shen, W. Pisula, M. Liang, L. Zhi and K. Müllen, *J. Am. Chem. Soc.*, 2009, **131**, 14618-14619.
89. X. Liu, B. He, Z. Xu, M. Yin, W. Yang, H. Zhang, J. Cao and J. Shen, *Nanoscale*, 2015, **7**, 445-449.
90. Y. Lu, B. He, J. Shen, J. Li, W. Yang and M. Yin, *Nanoscale*, 2015, **7**, 1606-1609.
91. A. M. Breul, M. D. Hager and U. S. Schubert, *Chem. Soc. Rev.*, 2013, **42**, 5366-5407.
92. X. Zhang, X. Zhang, K. Wang, H. Liu, Z. Gu, Y. Yang and Y. Wei, *J. Mater.Chem. C*, 2015, 10.1039/C1034TC02556C
93. K. Wang, X. Zhang, X. Zhang, B. Yang, Z. Li, Q. Zhang, Z. Huang and Y. Wei, *Macromol. Chem Phys*, 2015, 10.1002/macp.201400564.
94. K. Wang, X. Zhang, X. Zhang, B. Yang, Z. Li, Q. Zhang, Z. Huang and Y. Wei, *Polym. Chem.*, 2015, 10.1039/C1034PY01452A.
95. Z. Chen, X. Han, J. Zhang, D. Wu, G.-A. Yu, J. Yin and S. H. Liu, *RSC Adv.*, 2015, **5**, 15341-15349.
96. H. Tong, Y. Hong, Y. Dong, M. Häußler, J. W. Lam, Z. Li, Z. Guo, Z. Guo and B. Z. Tang, *Chem. Commun.*, 2006, 3705-3707.
97. X. Lou, C. W. T. Leung, C. Dong, Y. Hong, S. Chen, E. Zhao, J. W. Y. Lam and B. Z. Tang, *RSC Adv.*, 2014, **4**, 33307-33311.
98. A. Rananaware, R. S. Bhosale, H. Patil, M. Al Kobaisi, A. Abraham, R. Shukla, S. V. Bhosale and S. V. Bhosale, *RSC Adv.*, 2014, **4**, 59078-59082.
99. H. Deng, B. Liu, C. Yang, G. Li, Y. Zhuang, B. Li and X. Zhu, *RSC Adv.*, 2014, **4**, 62021-62029.
100. M. Baglan, S. Ozturk, B. Gür, K. Meral, U. Bozkaya, O. A. Bozdemir and S. Atılgan, *RSC Adv.*, 2013, **3**, 15866-15874.
101. P. Roy, D. Jana, A. Kundu and A. Pramanik, *RSC Adv.*, 2014, **4**, 62684-62688.
102. Y. Hong, J. W. Lam and B. Z. Tang, *Chem. Commun.*, 2009, 4332-4353.
103. S.-L. Deng, T.-L. Chen, W.-L. Chien and J.-L. Hong, *J. Mater. Chem. C*, 2014, **2**, 651-659.
104. C. Yu, Y. Wu, F. Zeng, X. Li, J. Shi and S. Wu, *Biomacromolecules*, 2013, **14**, 4507-4514.
105. X. Zhang, X. Zhang, B. Yang, Y. Zhang and Y. Wei, *ACS Appl. Mater. Inter.*, 2014, **6**, 3600-3606.
106. M. Liu, X. Zhang, B. Yang, F. Deng, Z. Li, J. Wei, X. Zhang and Y. Wei, *Appl. Surf. Sci.*, 2014, **322**, 155-161.
107. D. Ding, K. Li, B. Liu and B. Z. Tang, *Accounts Chem. Res.*, 2013, **46**, 2441-2453.
108. C. W. T. Leung, Y. Hong, S. Chen, E. Zhao, J. W. Y. Lam and B. Z. Tang, *J. Am. Chem. Soc.*, 2012, **135**, 62-65.
109. D. Wang, J. Qian, W. Qin, A. Qin, B. Z. Tang and S. He, *Sci. Rep.*, 2014, **4**.
110. J. Mei, Y. Hong, J. W. Lam, A. Qin, Y. Tang and B. Z. Tang, *Adv. Mater.*, 2014, **26**, 5429-5479.
111. J. Geng, K. Li, W. Qin, L. Ma, G. G. Gurzadyan, B. Z. Tang and B. Liu, *Small*, 2013, **9**, 2012-2019.
112. K. Li, D. Ding, Q. Zhao, J. Sun, B. Z. Tang and B. Liu, *Sci. China Chem.*, 2013, **56**, 1228-1233.
113. J. Geng, Z. Zhu, W. Qin, L. Ma, Y. Hu, G. G. Gurzadyan, B. Z. Tang and B. Liu, *Nanoscale*, 2014, **6**, 939-945.
114. H. Lu, F. Su, Q. Mei, Y. Tian, W. Tian, R. H. Johnson and D. R. Meldrum, *J. Mater. Chem.*, 2012, **22**, 9890-9900.
115. Z. Wang, L. Yan, L. Zhang, Y. Chen, H. Li, J. Zhang, Y. Zhang, X. Li, B. Xu and X. Fu, *Polymer Chem.*, 2014, **5**, 7013-7020.
116. B. Xu, J. Zhang, H. Fang, S. Ma, Q. Chen, H. Sun, C. Im and W. Tian, *Polym. Chem.*, 2014, **5**, 479-488.
117. C. Li and S. Liu, *Chem. Commun.*, 2012, **48**, 3262-3278.
118. C. Ma, Q. Ling, S. Xu, H. Zhu, G. Zhang, X. Zhou, Z. Chi, S. Liu, Y. Zhang and J. Xu, *Macromol. Biosci.*, 2014, **14**, 235-243.
119. C. Zhang, S. Jin, K. Yang, X. Xue, Z. Li, Y. Jiang, W.-Q. Chen, L. Dai, G. Zou and X.-J. Liang, *ACS Appl. Mater. Inter.*, 2014, **6**, 8971-8975.
120. X. Zhang, X. Zhang, L. Tao, Z. Chi, J. Xu and Y. Wei, *J. Mater. Chem. B*, 2014, **2**, 4398-4414.
121. R. T. Kwok, J. Geng, J. W. Lam, E. Zhao, G. Wang, R. Zhan, B. Liu and B. Z. Tang, *J. Mater. Chem. B*, 2014, **2**, 4134-4141.
122. D. Ding, J. Liang, H. Shi, R. T. Kwok, M. Gao, G. Feng, Y. Yuan, B. Z. Tang and B. Liu, *J. Mater. Chem. B*, 2014, **2**, 231-238.
123. H. Wu, H. Zhao, X. Song, S. Li, X. Ma and M. Tan, *J. Mater.Chem. B*, 2014, **2**, 5302-5308.
124. G. Yu, G. Tang and F. Huang, *J. Mater.Chem. C*, 2014, **2**, 6609-6617.
125. P. Alam, P. Das, C. Climent, M. Karanam, D. Casanova, A. Choudhury, P. Alemany, N. Jana and I. Laskar, *J. Mater. Chem. C*, 2014, **2**, 5615-5628.
126. Y. Lin, G. Chen, L. Zhao, W. Z. Yuan, Y. Zhang and B. Z. Tang, *J. Mater.Chem. C*, 2015, **3**, 112-120.
127. Y. Chen, J. W. Lam, S. Chen and B. Z. Tang, *J. Mater.Chem. C*, 2015, **2**, 6192-6198.
128. L. Kong, Y.-p. Tian, Q.-y. Chen, Q. Zhang, H. Wang, D.-q. Tan, Z.-m. Xue, J.-y. Wu, H.-p. Zhou and J.-x. Yang, *J. Mater. Chem. C*, 2015, **3**, 570-581.
129. G.-F. Zhang, Z.-Q. Chen, M. P. Aldred, Z. Hu, T. Chen, Z. Huang, X. Meng and M.-Q. Zhu, *Chem. Commun.*, 2014, **50**, 12058-12060.
130. X. Zhang, Z. Ma, Y. Yang, X. Zhang, X. Jia and Y. Wei, *J. Mater. Chem. C*, 2014, **2**, 8932-8938.
131. M. Liu, X. Zhang, B. Yang, F. Deng, Z. Huang, Y. Yang, Z. Li, X. Zhang and Y. Wei, *RSC Adv.*, 2014, **4**, 35137-35143.
132. X. Zhang, X. Zhang, B. Yang, J. Hui, M. Liu, Z. Chi, S. Liu, J. Xu and Y. Wei, *Polym. Chem.*, 2014, **5**, 683-688.
133. R.-H. Chien, C.-T. Lai and J.-L. Hong, *J. Phys. Chem. C*, 2011, **115**, 12358-12366.
134. R.-H. Chien, C.-T. Lai and J.-L. Hong, *Macromol. Chem. Phys.*, 2011, **213**, 666-677.
135. C.-M. Yang, Y.-W. Lai, S.-W. Kuo and J.-L. Hong, *Langmuir*, 2012, **28**, 15725-15735.
136. K.-Y. Shih, Y.-C. Lin, T.-S. Hsiao, S.-L. Deng, S.-W. Kuo and J.-L. Hong, *Polym. Chem.*, 2014, **5**, 5765-5774.
137. T.-S. Hsiao, S.-L. Deng, K.-Y. Shih and J.-L. Hong, *J. Mater. Chem. C*, 2014, **2**, 4828-4834.
138. S.-H. Huang, Y.-W. Chiang and J.-L. Hong, *Polym. Chem.*, 2015, **6**, 497-508.
139. S.-L. Deng, P.-C. Huang, L.-Y. Lin, D.-J. Yang and J.-L. Hong, *RSC Adv.*, 2015, **5**, 19512-19519.
140. T.-S. Hsiao, P.-C. Huang, L.-Y. Lin, D.-J. Yang and J.-L. Hong, *Polym. Chem.*, 2015, 10.1039/C1034PY01774A.
141. K.-Y. Shih, T.-S. Hsiao, S.-L. Deng and J.-L. Hong, *Macromolecules*, 2014, **47**, 4037-4047.
142. W.-C. Wu, C.-Y. Chen, Y. Tian, S.-H. Jang, Y. Hong, Y. Liu, R. Hu, B. Z. Tang, Y.-T. Lee, C.-T. Chen, W.-C. Chen and A. K.-Y. Jen, *Adv. Funct. Mater.*, 2010, **20**, 1413-1423.
143. X. Zhang, X. Zhang, S. Wang, M. Liu, L. Tao and Y. Wei, *Nanoscale*, 2013, **5**, 147-150.
144. Y. Zhang, Y. Chen, X. Li, J. Zhang, J. Chen, B. Xu, X. Fu and W. Tian, *Polym. Chem.*, 2014, **5**, 3824-3830.
145. H. Lu, X. Zhao, W. Tian, Q. Wang and J. Shi, *RSC Adv.*, 2014, **4**, 18460-18466.
146. X. Zhang, X. Zhang, B. Yang, S. Wang, M. Liu, Y. Zhang, L. Tao and Y. Wei, *RSC Adv.*, 2013, **3**, 9633-9636.
147. J. Geng, K. Li, D. Ding, X. Zhang, W. Qin, J. Liu, B. Z. Tang and B. Liu, *Small*, 2012, **8**, 3655-3663.
148. M. Li, Y. Hong, Z. Wang, S. Chen, M. Gao, R. T. Kwok, W. Qin, J. W. Lam, Q. Zheng and B. Z. Tang, *Macromol. Rapid Commun.*, 2013, **34**, 767-771.
149. X. Zhang, X. Zhang, B. Yang, M. Liu, W. Liu, Y. Chen and Y. Wei, *Polym. Chem.*, 2013, **4**, 4317-4321.
150. R. Zhang, Y. Yuan, J. Liang, R. T. Kwok, Q. Zhu, G. Feng, J. Geng, B. Z. Tang and B. Liu, *ACS Appl. Mater. Inter.*, 2014, **6**, 14302-14310.
151. T. Borase, M. Iacono, S. I. Ali, P. D. Thornton and A. Heise, *Polym. Chem.*, 2012, **3**, 1267-1275.
152. M. E. Levere, N. H. Nguyen, H.-J. Sun and V. Percec, *Polym. Chem.*, 2013, **4**, 686-694.

153. T. Liu, D. Zhang, X. Yang and C. Li, *Polym. Chem.*, 2015, **6**, 1512-1520.
154. Z. Liu, S. Zhu, Y. Li, Y. Li, P. Shi, Z. Huang and X. Huang, *Polym. Chem.*, 2015, 10.1039/C1034PY00903G.
155. G. Marcelo, A. Munoz-Bonilla, J. Rodriguez-Hernandez and M. Fernandez-Garcia, *Polym. Chem.*, 2013, **4**, 558-567.
156. N. H. Nguyen, J. Kulis, H.-J. Sun, Z. Jia, B. Van Beusekom, M. E. Levere, D. A. Wilson, M. J. Monteiro and V. Percec, *Polym. Chem.*, 2013, **4**, 144-155.
157. S. R. Samanta, H.-J. Sun, A. Anastasaki, D. M. Haddleton and V. Percec, *Polym. Chem.*, 2014, **5**, 89-95.
158. C. Waldron, A. Anastasaki, R. McHale, P. Wilson, Z. Li, T. Smith and D. M. Haddleton, *Polym. Chem.*, 2014, **5**, 892-898.
159. C. Waldron, Q. Zhang, Z. Li, V. Nikolaou, G. Nurumbetov, J. Godfrey, R. McHale, G. Yilmaz, R. K. Randev and M. Girault, *Polym. Chem.*, 2014, **5**, 57-61.
160. Q. Wan, M. Liu, J. Tian, F. Deng, G. Zeng, Z. Li, K. Wang, Q. Zhang, X. Zhang and Y. Wei, *Polym. Chem.*, 2015, **6**, 1786-1792.
161. P. Xiang, K. Petrie, M. Kontopoulou, Z. Ye and R. Subramanian, *Polym. Chem.*, 2013, **4**, 1381-1395.
162. B. Yang, Y. Zhao, X. Ren, X. Zhang, C. Fu, Y. Zhang, Y. Wei and L. Tao, *Polym. Chem.*, 2015, **6**, 509-513.
163. Q. Zhang, A. Anastasaki, G.-Z. Li, A. J. Haddleton, P. Wilson and D. M. Haddleton, *Polym. Chem.*, 2014, **5**, 3876-3883.
164. X. Zhang, S. Wang, C. Fu, L. Feng, Y. Ji, L. Tao, S. Li and Y. Wei, *Polym. Chem.*, 2012, **3**, 2716-2719.
165. X. Zhang, X. Zhang, B. Yang, J. Hui, M. Liu, W. Liu, Y. Chen and Y. Wei, *Polym. Chem.*, 2014, **5**, 689-693.
166. X. Zhang, J. Ji, X. Zhang, B. Yang, M. Liu, W. Liu, L. Tao, Y. Chen and Y. Wei, *RSC Adv.*, 2013, **3**, 21817-21823.
167. X. Zhang, M. Liu, Y. Zhang, B. Yang, Y. Ji, L. Feng, L. Tao, S. Li and Y. Wei, *RSC Adv.*, 2012, **2**, 12153-12155.
168. X.-f. Zhang, Y. Wu, J. Huang, X.-l. Miao, Z.-b. Zhang and X. Zhu, *Chinese J. Polym. Sci.*, 2013, **31**, 702-712.
169. J.-l. Pan, Z. Li, L.-f. Zhang, Z.-p. Cheng and X.-l. Zhu, *Chinese J. Polym. Sci.*, 2014, **32**, 1010-1018.
170. L.-b. Bai, R.-r. Zheng, W.-l. Li, Y.-g. Wu, X.-w. Ba and H.-j. Wang, *Chinese J. Polym. Sci.*, 2013, **31**, 1038-1045.
171. Y.-h. Wang, D. Xiang, R. Ren, J. Luo, W.-l. Sun and Z.-q. Shen, *Chinese J. Polym. Sci.*, 2014, **32**, 1500-1506.
172. P. Ren, Y.-b. Wu, W.-l. GUO, S.-x. Li and Y. Chen, *Chinese J. Polym. Sci.*, 2013, **31**, 285-293.
173. G.-s. Wang, L. Wang, Z.-y. Wei, L. Sang, X.-f. Dong, M. Qi, G.-y. Chen, Y. Chang and W.-x. Zhang, *Chinese J. Polym. Sci.*, 2013, **31**, 1011-1021.
174. H. Lu, F. Su, Q. Mei, X. Zhou, Y. Tian, W. Tian, R. H. Johnson and D. R. Meldrum, *J. Polym. Sci. Polym. Chem.*, 2012, **50**, 890-899.
175. Y.-W. Lai, S.-W. Kuo and J.-L. Hong, *RSC Adv.*, 2012, **2**, 8194-8200.
176. C.-M. Yang, I.-W. Lee, T.-L. Chen, W.-L. Chien and J.-L. Hong, *J. Mater. Chem. C*, 2013, **1**, 2842-2850.
177. S.-T. Li, Y.-C. Lin, S.-W. Kuo, W.-T. Chuang and J.-L. Hong, *Polym. Chem.*, 2012, **3**, 2393-2402.
178. C. T. Lai and J. L. Hong, *J. Mater.Chem.*, 2012, **22**, 9546-9555.
179. C.-T. Lai and J.-L. Hong, *J. Phys. Chem. B*, 2010, **114**, 10302-10310.
180. W.-L. Chien, C.-M. Yang, T.-L. Chen, S.-T. Li and J.-L. Hong, *RSC Adv.*, 2010, **3**, 6930-6938.
181. R.-H. Chien, C.-T. Lai and J.-L. Hong, *J. Phys. Chem. C*, 2011, **115**, 20732-20739.
182. C.-T. Lai, R.-H. Chien, S.-W. Kuo and J.-L. Hong, *Macromolecules*, 2011, **44**, 6546-6556.
183. R.-H. Chien, C.-T. Lai and J.-L. Hong, *J. Phys. Chem. C*, 2011, **115**, 5958-5965.
184. X. Ren, B. Yang, Y. Zhao, X. Zhang, X. Wang, Y. Wei and L. Tao, *Polymer*, 2015, 10.1016/j.polymer.2015.1002.1033.
185. H. Li, X. Zhang, X. Zhang, K. Wang, Q. Zhang and Y. Wei, *J. Mater. Chem. B*, 2015, **3**, 1193-1197.
186. L. Xu, N. Liu, Y. Cao, F. Lu, Y. Chen, X. Zhang, L. Feng and Y. Wei, *ACS Appl. Mater. Inter.*, 2014, **6**, 13324-13329.
187. X. Zhang, X. Zhang, B. Yang, Y. Zhang and Y. Wei, *Tetrahedron*, 2014, **70**, 3553-3559.
188. X. Zhang, Z. Ma, Y. Yang, X. Zhang, Z. Chi, S. Liu, J. Xu, X. Jia and Y. Wei, *Tetrahedron*, 2014, **70**, 924-929.
189. X. Zhang, X. Zhang, B. Yang, L. Liu, F. Deng, J. Hui, M. Liu, Y. Chen and Y. Wei, *RSC Adv.*, 2014, **4**, 24189-24193.
190. X. Zhang, M. Liu, B. Yang, X. Zhang, Z. Chi, S. Liu, J. Xu and Y. Wei, *Polym. Chem.*, 2013, **4**, 5060-5064.
191. X. Zhang, C. Fu, L. Feng, Y. Ji, L. Tao, Q. Huang, S. Li and Y. Wei, *Polymer*, 2012, **53**, 3178-3184.
192. X. Zhang, Y. Zhu, J. Li, Z. Zhu, J. Li, W. Li and Q. Huang, *J. Nanopart. Res.*, 2011, **13**, 6941-6952.
193. X. Zhang, X. Zhang, B. Yang, M. Liu, W. Liu, Y. Chen and Y. Wei, *Polym. Chem.*, 2014, **5**, 399-404.
194. X. Zhang, X. Zhang, B. Yang, M. Liu, W. Liu, Y. Chen and Y. Wei, *Polym. Chem.*, 2014, **5**, 356-360.
195. Z. Huang, X. Zhang, X. Zhang, C. Fu, K. Wang, J. Yuan, L. Tao and Y. Wei, *Polym. Chem.*, 2015, **6**, 607-612.
196. H. Li, X. Zhang, X. Zhang, B. Yang, Y. Yang and Y. Wei, *Polym. Chem.*, 2014, **5**, 3758-3762.
197. H. Li, X. Zhang, X. Zhang, B. Yang, Y. Yang, Z. Huang and Y. Wei, *Macromol. Biosci.*, 2014, **14**, 1361-1367.
198. H. Li, X. Zhang, X. Zhang, B. Yang, Y. Yang and Y. Wei, *Macromolecul. Rapid Comm.*, 2014, **35**, 1661-1667.
199. K. Wang, X. Zhang, X. Zhang, B. Yang, Z. Li, Q. Zhang, Z. Huang and Y. Wei, *J. Mater. Chem. C*, 2015.
200. M. Liu, X. Zhang, B. Yang, F. Deng, Y. Yang, Z. Li, X. Zhang and Y. Wei, *Macromol. Biosci.*, 2014, **14**, 1712-1718.
201. H. Li, X. Zhang, X. Zhang, B. Yang, Y. Yang and Y. Wei, *Polym.Chem.*, 2014, **5**, 3758-3762.
202. C. Ma, X. Zhang, K. Wang, x. zhang, Y. Zhou, H. Liu and y. wei, *Polym. Chem.*, 2015, 10.1039/C1035PY00111K.
203. Y. Zhao, Y. Wu, G. Yan and K. Zhang, *RSC Adv.*, 2014, **4**, 51194-51200.
204. M. Liu, X. Zhang, B. Yang, L. Liu, F. Deng, X. Zhang and Y. Wei, *Macromol. Biosci.*, 2014, **14**, 1260-1267.
205. H. Li, X. Zhang, X. Zhang, B. Yang and Y. Wei, *Colloids Surf. B Biointerfaces*, 2014, **121**, 347-353.
206. D.-h. Gao, M.-q. Jia and Y. Luo, *Chinese J. Polym. Sci.*, 2013, **31**, 974-983.
207. Z.-m. Liu, Y. Liu, N.-p. He and B.-y. Li, *Chinese J. Polym. Sci.*, 2014, **32**, 1602-1609.
208. F. Mahtab, J. W. Lam, Y. Yu, J. Liu, W. Yuan, P. Lu and B. Z. Tang, *Small*, 2011, **7**, 1448-1455.
209. Z. Wang, B. Xu, L. Zhang, J. Zhang, T. Ma, J. Zhang, X. Fu and W. Tian, *Nanoscale*, 2013, **5**, 2065-2072.
210. D. Li, J. Yu and R. Xu, *Chem. Commun.*, 2011, **47**, 11077-11079.
211. M. Li, J. W. Lam, F. Mahtab, S. Chen, W. Zhang, Y. Hong, J. Xiong, Q. Zheng and B. Z. Tang, *J. Mater. Chem. B*, 2013, **1**, 676-684.
212. L. Aparicio-Ixta, G. Ramos-Ortiz, J. L. Pichardo-Molina, J. L. Maldonado, M. Rodríguez, V. M. Tellez-Lopez, D. Martinez-Fong, M. G. Zolotukhin, S. Fomine and M. A. Meneses-Nava, *Nanoscale*, 2012, **4**, 7751-7759.
213. F. Mahtab, Y. Yu, J. W. Lam, J. Liu, B. Zhang, P. Lu, X. Zhang and B. Z. Tang, *Adv. Funct. Mater.*, 2011, **21**, 1733-1740.
214. Y. Xia, M. Li, T. Peng, W. Zhang, J. Xiong, Q. Hu, Z. Song and Q. Zheng, *Int. J. Mol. Sci.*, 2013, **14**, 1080-1092.
215. S. Yao, A. Shao, W. Zhao, S. Zhu, P. Shi, Z. Guo, W. Zhu and J. Shi, *RSC Adv.*, 2014, **4**, 58976-58981.
216. C. Miao, D. Li, Y. Zhang, J. Yu and R. Xu, *Micropor. Mesopor. Mat.*, 2014, **196**, 46-50.
217. X. Wang, A. R. Morales, T. Urakami, L. Zhang, M. V. Bondar, M. Komatsu and K. D. Belfield, *Bioconjugate Chem.*, 2011, **22**, 1438-1450.
218. R.-r. Zhang, L. Li, L.-l. Tong and B. Tang, *Nanotechnology*, 2013, **24**, 015604.
219. Z. Zhu, X. Zhao, W. Qin, G. Chen, J. Qian and Z. Xu, *Sci. China Chem.*, 2013, **56**, 1247-1252.
220. M. Faisal, Y. Hong, J. Liu, Y. Yu, J. W. Lam, A. Qin, P. Lu and B. Z. Tang, *Chem-Eur. J.*, 2011, **16**, 4266-4272.
221. D. Li, C. Miao, X. Wang, X. Yu, J. Yu and R. Xu, *Chem. Commun.*, 2013, **49**, 9549-9551.

222. D. Li, Z. Liang, J. Chen, J. Yu and R. Xu, *Dalton Trans.*, 2013, **42**, 9877-9883.
223. D. Li, Y. Zhang and B. Zhou, *J. Solid State Chem.*, 2015, **225**, 427-430.
224. X. Zhang, X. Zhang, B. Yang, L. Liu, J. Hui, M. Liu, Y. Chen and Y. Wei, *RSC Adv.*, 2014, **4**, 10060-10066.
225. N.-n. Zhao, W. Nie, J. Mao, W.-c. Wang and X.-l. Ji, *Chinese J. Polym. Sci.*, 2013, **31**, 1233-1241.
226. Y. Zhang, X.-j. Wang, M. Guo, H.-S. Yan, C.-h. Wang and K.-l. Liu, *Chinese J. Polym. Sci.*, 2013, **32**, 1329-1337.
227. N. Li, Y. Jin, L.-z. Xue, P.-l. Li, D.-y. Yan and X.-y. Zhu, *Chinese J. Polym. Sci.*, 2013, **31**, 530-540.
228. F.-m. Gong, Z.-q. Zhang, X.-d. Chen, L. Zhang, X.-s. Yu, Q.-h. Yang, X.-t. Shuai, B.-l. Liang and D. Cheng, *Chinese J. Polym. Sci.*, 2014, **32**, 321-332.
229. L.-z. Zhang, Y.-j. Zhang, W. Wu and X.-q. Jiang, *Chinese J. Polym. Sci.*, 2013, **31**, 778-786.
230. X. Zhang, J. Yin, C. Peng, W. Hu, Z. Zhu, W. Li, C. Fan and Q. Huang, *Carbon*, 2011, **49**, 986-995.
231. Y. Zhu, W. Li, Q. Li, Y. Li, Y. Li, X. Zhang and Q. Huang, *Carbon*, 2009, **47**, 1351-1358.
232. X. Zhang, J. Yin, C. Kang, J. Li, Y. Zhu, W. Li, Q. Huang and Z. Zhu, *Toxicol. Lett.*, 2010, **198**, 237-243.
233. Z. Lin, H. Zhang, J. Huang, Z. Xi, L. Liu and B. Lin, *Toxicol. Res.*, 2014, **3**, 497-502.
234. X. Cai, J. Hao, X. Zhang, B. Yu, J. Ren, C. Luo, Q. Li, Q. Huang, X. Shi and W. Li, *Toxicol. Appl. Pharmacol.*, 2010, **243**, 27-34.
235. X. Zhang, W. Hu, J. Li, L. Tao and Y. Wei, *Toxicol. Res.*, 2012, **1**, 62-68.
236. L. Zhan, G. Yanxia, Z. Xiaoyong, Q. Wei, F. Qiaohui, L. Yan, J. Zongxian, W. Jianjun, T. Yuqin and D. Xiaojiang, *J. Nanopart. Res.*, 2011, **13**, 2939-2947.
237. Y. Zhu, X. Zhang, J. Zhu, Q. Zhao, Y. Li, W. Li, C. Fan and Q. Huang, *Int. J. Mol. Sci.*, 2012, **13**, 12336-12348.
238. J. Liang, R. T. K. Kwok, H. Shi, B. Z. Tang and B. Liu, *ACS Appl. Mater. Inter.*, 2013, **5**, 8784-8789.
239. Y. Yuan, R. T. Kwok, G. Feng, J. Liang, J. Geng, B. Z. Tang and B. Liu, *Chem. Commun.*, 2014, **50**, 295-297.
240. H. Lu, B. Xu, Y. Dong, F. Chen, Y. Li, Z. Li, J. He, H. Li and W. Tian, *Langmuir*, 2010, **26**, 6838-6844.
241. X. Li, S. Zhu, B. Xu, K. Ma, J. Zhang, B. Yang and W. Tian, *Nanoscale*, 2013, **5**, 7776-7779.
242. M. Gao, Q. Hu, G. Feng, B. Z. Tang and B. Liu, *J. Mater. Chem. B*, 2014, **2**, 3438-3442.
243. C. Yin, W. Song, R. Jiang, X. Lu, W. Hu, Q. Shen, X. Li, J. Li, Q. Fan and W. Huang, *Polym. Chem.*, 2014, **5**, 5598-5608.
244. Z. Huang, X. Zhang, X. Zhang, B. Yang, Y. Zhang, K. Wang, J. Yuan, L. Tao and Y. Wei, *Polym. Chem.*, 2015, **6**, 2133-2138.
245. K. Wang, X. Zhang, X. Zhang, B. Yang, Z. Li, Q. Zhang, Z. Huang and Y. Wei, *J. Mater. Chem. C*, 2015, **3**, 1854-1860.
246. X. Zhang, X. Zhang, K. Wang, H. Liu, Z. Gu, Y. Yang and Y. Wei, *J. Mater. Chem. C*, 2015, **3**, 1738-1744.
247. K. Wang, X. Zhang, X. Zhang, B. Yang, Z. Li, Q. Zhang, Z. Huang and Y. Wei, *Polym. Chem.*, 2015, **6**, 1360-1366.
248. Y. Gao, Y. Qu, T. Jiang, H. Zhang, N. He, B. Li, J. Wu and J. Hua, *J. Mater. Chem. C*, 2014, **2**, 6353-6361.
249. S. Li, Y. Shang, E. Zhao, R. T. Kwok, J. W. Y. Lam, Y. Song and B. Z. Tang, *J. Mater. Chem. C*, 2015, 10.1039/C1034TC02691H
250. W. Qin, D. Ding, J. Liu, W. Z. Yuan, Y. Hu, B. Liu and B. Z. Tang, *Adv. Funct. Mater.*, 2012, **22**, 771-779.
251. S. Liu, H. Sun, Y. Ma, S. Ye, X. Liu, X. Zhou, X. Mou, L. Wang, Q. Zhao and W. Huang, *J. Mater. Chem.*, 2012, **22**, 22167-22173.
252. K. Li, W. Qin, D. Ding, N. Tomczak, J. Geng, R. Liu, J. Liu, X. Zhang, H. Liu and B. Liu, *Sci. Rep.*, 2013, **3**, 10.1038/srep01150.
253. Z. Wang, S. Chen, J. W. Lam, W. Qin, R. T. Kwok, N. Xie, Q. Hu and B. Z. Tang, *J. Am. Chem. Soc.*, 2013, **135**, 8238-8245.
254. Y. Yu, C. Feng, Y. Hong, J. Liu, S. Chen, K. M. Ng, K. Q. Luo and B. Z. Tang, *Adv. Mater.*, 2011, **23**, 3298-3302.
255. E. Zhao, Y. Hong, S. Chen, C. W. Leung, C. Y. Chan, R. T. Kwok, J. W. Lam and B. Z. Tang, *Adv. Healthc. Mater.*, 2014, **3**, 88-96.
256. H. Li, X. Zhang, X. Zhang, K. Wang, H. Liu and Y. Wei, *ACS Appl. Mater. Inter.*, 2015, **7**, 4241-4246.
257. G. Feng, C. Y. Tay, Q. X. Chui, R. Liu, N. Tomczak, J. Liu, B. Z. Tang, D. T. Leong and B. Liu, *Biomaterials*, 2014, **35**, 8669-8677.
258. K. Li, Z. Zhu, P. Cai, R. Liu, N. Tomczak, D. Ding, J. Liu, W. Qin, Z. Zhao and Y. Hu, *Chem. Mater.*, 2013, **25**, 4181-4187.
259. D. Ding, G. Wang, J. Liu, K. Li, K. Pu, Y. Hu, J. C. Ng, B. Z. Tang and B. Liu, *Small*, 2012, **8**, 3523-3530.
260. J. Zhang, C. Li, X. Zhang, S. Huo, S. Jin, F.-F. An, X. Wang, X. Xue, C. Okeke and G. Duan, *Biomaterials*, 2015, **42**, 103-111.
261. X. Zhang, M. Liu, X. Zhang, F. Deng, C. Zhou, J. Hui, W. Liu and Y. Wei, *Toxicol. Res.*, 2015, **4**, 160-168.
262. J. Yin, C. Kang, Y. Li, Q. Li, X. Zhang and W. Li, *Toxicol. Res.*, 2014, **3**, 367-374.
263. B. Li, X.-Y. Zhang, J.-Z. Yang, Y.-J. Zhang, W.-X. Li, C.-H. Fan and Q. Huang, *Int. J. Nanomed.*, 2014, **9**, 4697-4707.
264. Y. Li, H. Yu, Y. Qian, J. Hu and S. Liu, *Adv. Mater.*, 201, **26**, 6734-6741.
265. K. Li, D. Ding, C. Prashant, W. Qin, C.-T. Yang, B. Z. Tang and B. Liu, *Adv. healthc. Mater.*, 2013, **2**, 1600-1605.
266. H. Tong, Y. Hong, Y. Dong, M. Häussler, Z. Li, J. W. Lam, Y. Dong, H. H.-Y. Sung, I. D. Williams and B. Z. Tang, *J. Phys. Chem. B*, 2007, **111**, 11817-11823.
267. H. Shi, J. Liu, J. Geng, B. Z. Tang and B. Liu, *J. Am. Chem. Soc.*, 2012, **134**, 9569-9572.
268. Y. Hong, L. Meng, S. Chen, C. W. T. Leung, L.-T. Da, M. Faisal, D.-A. Silva, J. Liu, J. W. Y. Lam and X. Huang, *J. Am. Chem. Soc.*, 2012, **134**, 1680-1689.
269. H. Shi, R. T. Kwok, J. Liu, B. Xing, B. Z. Tang and B. Liu, *J. Am. Chem. Soc.*, 2012, **134**, 17972-17981.
270. X. Lou, Y. Hong, S. Chen, C. W. T. Leung, N. Zhao, B. Situ, J. W. Y. Lam and B. Z. Tang, *Sci. Rep.*, 2014, **4**, 10.1038/srep04272.
271. Y. Li, R. T. Kwok, B. Z. Tang and B. Liu, *RSC Adv.*, 2013, **3**, 10135-10138.
272. Z. Song, Y. Hong, R. T. Kwok, J. W. Lam, B. Liu and B. Z. Tang, *J. Mater. Chem. B*, 2014, **2**, 1717-1723.
273. M. Gao, C. K. Sim, C. W. T. Leung, Q. Hu, G. Feng, F. Xu, B. Z. Tang and B. Liu, *Chem. Commun.*, 2014, **50**, 8312-8315.
274. H. Shi, N. Zhao, D. Ding, J. Liang, B. Z. Tang and B. Liu, *Org. Biomol. Chem.*, 2013, **11**, 7289-7296.
275. Z. Song, R. T. Kwok, E. Zhao, Z. He, Y. Hong, J. W. Lam, B. Liu and B. Z. Tang, *ACS Appl. Mater. Inter.*, 2014, **6**, 17245-17254.
276. D. Ding, D. Mao, K. Li, X. Wang, W. Qin, R. Liu, D. S. Chiam, N. Tomczak, Z. Yang and B. Z. Tang, *ACS Nano*, 2014, **8**, 12620-12631.
277. Z. Wang, K. Ma, B. Xu, X. Li and W. Tian, *Sci.China Chem.*, 2013, **56**, 1234-1238.
278. X. Wang, J. Hu, T. Liu, G. Zhang and S. Liu, *J. Mater. Chem.*, 2012, **22**, 8622-8628.
279. X. Wang, J. Hu, G. Zhang and S. Liu, *J. Am. Chem. Soc.*, 2014, **136**, 9890-9893.
280. Y. Li, X. Hu, S. Tian, Y. Li, G. Zhang, G. Zhang and S. Liu, *Biomaterials*, 2014, **35**, 1618-1626.
281. S. Chen, Y. Hong, J. Liu, N.-W. Tseng, Y. Liu, E. Zhao, J. W. Yip Lam and B. Z. Tang, *J. Mater. Chem. B*, 2014, **2**, 3919-3923.
282. N. Zhao, M. Li, Y. Yan, J. W. Lam, Y. L. Zhang, Y. S. Zhao, K. S. Wong and B. Z. Tang, *J. Mater.Chem. C*, 2013, **1**, 4640-4646.
283. G. Liu, M. Yang, L. Wang, J. Zheng, H. Zhou, J. Wu and Y. Tian, *J. Mater. Chem. C*, 2014, **2**, 2684-2691.
284. R. Hu, J. W. Lam, J. Liu, H. H. Sung, I. D. Williams, Z. Yue, K. S. Wong, M. M. Yuen and B. Z. Tang, *Polym. Chem.*, 2012, **3**, 1481-1489.
285. H. Liu, Z. Lv, K. Ding, X. Liu, L. Yuan, H. Chen and X. Li, *J. Mater. Chem. B*, 2013, **1**, 5550-5556.
286. J. Liang, H. Shi, R. T. Kwok, M. Gao, Y. Yuan, W. Zhang, B. Z. Tang and B. Liu, *J. Mater. Chem. B*, 2014, **2**, 4363-4370.
287. Y. Yuan, R. T. Kwok, B. Z. Tang and B. Liu, *J. Am. Chem. Soc.*, 2014, **136**, 2546-2554.
288. Y. Yuan, G. Feng, W. Qin, B. Z. Tang and B. Liu, *Chem. Commun.*, 2014, **50**, 8757-8760.

289. Y. Yuan, Y. Chen, B. Z. Tang and B. Liu, *Chem. Commun.*, 2014, **50**, 3868-3870.
290. Y. Yuan, R. T. Kwok, R. Zhang, B. Z. Tang and B. Liu, *Chem. Commun.*, 2014, **50**, 11465-11468.
291. M. Gao, Q. Hu, G. Feng, N. Tomczak, R. Liu, B. Xing, B. Z. Tang and B. Liu, *Adv. Healthc. Mater.*, 2015, 10.1002/adhm.201400654.
292. D. Ding, R. T. Kwok, Y. Yuan, G. Feng, B. Z. Tang and B. Liu, *Mater. Horizons*, 2015, **2**, 100-105.
293. Y. Yuan, C.-J. Zhang, M. Gao, R. Zhang, B. Z. Tang and B. Liu, *Angew. Chem. Int. Ed.*, 2015, **54**, 1780-1786.
294. X. Xue, S. Jin, C. Zhang, K. Yang, S. Huo, F. Chen, G. Zou and X.-J. Liang, *ACS nano*, 2015.
295. M.-C. Hsieh, C.-H. Chien, C.-C. Chang and T.-C. Chang, *J. Mater.Chem.B*, 2013, **1**, 2350-2357.
296. D. Ding, J. Liang, H. Shi, R. T. Kwok, M. Gao, G. Feng, Y. Yuan, B. Z. Tang and B. Liu, *J. Mater.Chem. B*, 2014, **2**, 231-238.
297. Y. Yuan, R. T. Kwok, B. Z. Tang and B. Liu, *J. Am. Chem. Soc.* , 2014, **136**, 2546-2554.
298. X. Xue, Y. Zhao, L. Dai, X. Zhang, X. Hao, C. Zhang, S. Huo, J. Liu, C. Liu and A. Kumar, *Adv. Mater.*, 2014, **26**, 712-717.
299. X. Zhang, X. Zhang, S. Wang, M. Liu, Y. Zhang, L. Tao and Y. Wei, *ACS Appl. Mater. Inter.*, 2013, **5**, 1943-1947.